A finite rotation shell theory with application to composite structures

Friedrich Gruttmann — Sven Klinkel — Werner Wagner

Institut für Baustatik
Universität Karlsruhe
Kaiserstraße 12
76131 Karlsruhe, Germany

ABSTRACT. *In this paper we derive a finite element formulation for geometrical nonlinear shell structures. The formulation bases on a direct introduction of the isoparametric finite element formulation into the shell equations. The element allows the occurence of finite rotations which are described by a rotation tensor. A layerwise linear elastic material model for composites is chosen. The consistent linearization of all equations leads to quadratic convergence behaviour within the nonlinear solution procedure. Examples show the applicability and effectivity of the developed element.*

RÉSUMÉ. *Dans cet article nous proposons une formulation en éléments finis du comportement géométriquement non linéaire des coques. La formulation est basée sur l'introduction directe des interpolations isoparamétriques dans les équations gouvernantes. L'élément de coque peut être utilisé en présence de grandes rotations, qui sont représentées par le tenseur de rotation. La modélisation du comportement du matériau composite se fait par couche comme élastique linéaire. La linéarisation cohérente des équations gouvernantes conduit au taux de convergence quadratique de la résolution du système d'équations non linéaires. Quelques exemples numériques montrent l'applicabilité et l'efficacité de cet élément.*

KEY WORDS : *nonlinear shell formulation, finite rotations, composite material.*
MOTS-CLÉS : *formulation non linéaire de coques, rotations finies, matériau composite.*

Revue européenne des éléments finis. Volume 4 - n° 5-6/1995, pages 597 à 631

1 Introduction

In this paper we discuss the geometrical nonlinear behaviour of composite shell structures in the presence of finite rotations within the finite element method.

The application of composite materials became very popular in the last decades, especially in aircraft industries. The advantages of these materials are high strength and stiffness ratios coupled with a low specific weight. Thus, composites are used in highly loaded light weight structures. Often the designed constructions are thin shells which are very sensitive against loss of stability. Therefore the discussion of the stability behaviour is crucial for composite shell problems besides the description of material phenomena like matrix and fiber cracking or delamination. Due to these problems we have high requirements on the accuracy of the numerical calculations.

For this purpose we present a general shell element which includes the geometrical nonlinear effects, especially finite rotations in an exact manner. Up to now a number of general finite shell elements including finite rotations are known. We mention the formulations in [RAM77],[RAM76], [HUL81], [SIM90], [SPH86], [GSW89], [WRG93],[WRG90], [IBR94], [PAR91], [GEB90], [SCH86], [STM89], [BDM92], [DOR90] among others.

In this paper the derived element formulation is based on a Lagrangian description with Green-Lagrangian strains which are defined only by the deformed and undeformed base vectors of the shell mid–surface. The displacements are introduced with respect to the Cartesian base system. In this case a straight forward isoparametric formulation of the displacement field is possible, see e.g. [SIM90], [WAS93]. Hence, no shell specific formulations like e.g. Christoffel tensors are necessary. The components of the deformed and undeformed director are given with respect to the Cartesian coordinate system using an orthogonal transformation. All necessary matrices and vectors are calculated by standard linearization procedures acting on the base vectors and the directors. A simple formulation comes out for the tangent stiffness matrix and the residual used in the nonlinear finite element analysis.

The composite material description is given with respect to local material axis and a transformation to global directions is performed on the element level. Standard procedures are used to modify the general 3D-material law for the two-dimensional case on the shell mid–surface.

Examples show the applicability of the proposed element for geometrical highly nonlinear shell structures of composite material.

The contents of the paper may be outlined as follows: The second section shows the basic kinematic assumptions whereas in the third section the material law for a composite shell formulation is discussed. Based on the weak form in the fourth section, the associated finite element formulation is given in section 5. Finally we show some illustrative examples in the last section.

2 Kinematics

The mathematical description of a point $P \in \mathcal{B}$ in shell space is based on the introduction of the position vector $\mathbf{p}$, which is a function of the convected coordinates $\Theta^i = \xi, \eta, \zeta$, see Figure 1. We have to distinguish between quantities in the reference configuration and the current configuration (marked by an upper bar). Thus the position of the points $\bar{P} \in \bar{\mathcal{B}}$ and $P \in \mathcal{B}$ is given by

$$\mathbf{p} = \mathbf{x} + \zeta\, \mathbf{a}_3\,, \qquad \bar{\mathbf{p}} = \bar{\mathbf{x}} + \zeta\, \mathbf{d}\,, \qquad -\frac{h}{2} \le \zeta \le +\frac{h}{2}\,. \tag{1}$$

In (1) $\bar{\mathbf{x}}$ is the position vector to the shell mid-surface $\zeta = 0$ and $\mathbf{d}$ a director vector which is fundamental to characterize the rotational behaviour. $\mathbf{d}$ is in general not perpendicular to the deformed mid-surface if we introduce a so called Reissner–Mindlin theory. In the special case that $\mathbf{d}$ coincides with the normal vector $\bar{\mathbf{a}}_3$, this kinematic assumption leads to the Kirchoff–Love theory where transverse shear deformations are neglected.

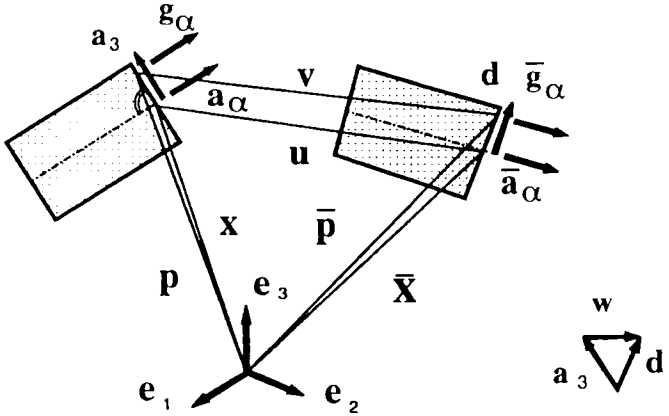

Figure 1: *Kinematic of a thin shell*

The following quantities are necessary to describe the geometry of the shell in the reference configuration.

base vectors	$\mathbf{a}_i = \{\mathbf{a}_\alpha, \mathbf{a}_3\}$:	$\mathbf{a}_\alpha$	=	$\mathbf{x}_{,\alpha}$
		$\mathbf{a}_3$	=	$\mathbf{a}_1 \times \mathbf{a}_2 / \lVert \mathbf{a}_1 \times \mathbf{a}_2 \rVert$
metric tensor:		$\mathbf{A}$	=	$\mathbf{a}_\alpha \otimes \mathbf{a}^\alpha$
curvature tensor:		$\mathbf{B}$	=	$-\mathbf{a}_{3,\alpha} \otimes \mathbf{a}^\alpha$
unit tensor:		$\mathbf{1}$	=	$\mathbf{a}_\alpha \otimes \mathbf{a}^\alpha + \mathbf{a}_3 \otimes \mathbf{a}_3$
base vectors in $\mathcal{B}$	$\mathbf{g}_i = \{\mathbf{g}_\alpha, \mathbf{g}_3\}$:	$\mathbf{g}_\alpha$	=	$\mathbf{a}_\alpha + \zeta \mathbf{a}_{3,\alpha}$
		$\mathbf{g}_3$	=	$\mathbf{a}_3$

(2)

The associated kinematic quantities of the current configuration are defined in the same way. In addition to the convected basis $\mathbf{g}_i$ the reciprocal basis $\mathbf{g}^i$ is given by the standard relation $\mathbf{g}_i \cdot \mathbf{g}^k = \delta_i{}^k$. For the relation between base vectors in shell space $\mathcal{B}$ and on the shell mid–surface $\mathcal{M}$ we introduce the shifter tensor $\mathbf{Z}$

$$\mathbf{g}_i = \mathbf{Z}\,\mathbf{a}_i \qquad\qquad \mathbf{g}^i = \mathbf{Z}^{T-1}\mathbf{a}^i\,, \tag{3}$$

with the standard definition of the shifter tensor

$$\mathbf{Z} = \mathbf{1} - \zeta\,\mathbf{B}\,. \tag{4}$$

For the calculation of strain measures we make use of the deformation gradient $\mathbf{F}$ which is defined in convected coordinates by

$$\mathbf{F} = \frac{\partial \mathrm{p}}{\partial \theta^k} \otimes \mathbf{g}^k = \bar{\mathbf{g}}_k \otimes \mathbf{g}^k = F_{ik}\,\mathbf{g}^i \otimes \mathbf{g}^k\,, \tag{5}$$

with the components of $\mathbf{F}$

$$F_{ik} = \mathbf{g}_i \cdot \bar{\mathbf{g}}_k\,. \tag{6}$$

The strain measures for our shell problem can now be obtained from the three–dimensional theory using the Green–Lagrangian strain tensor $\mathbf{E}_{\mathcal{B}} = \frac{1}{2}(\mathbf{F}^T\mathbf{F} - \mathbf{1})$. With eq. (5) $\mathbf{E}_{\mathcal{B}}$ can be stated in terms of the base vectors

$$\mathbf{E}_{\mathcal{B}} = E_{ik}\,\mathbf{g}^i \otimes \mathbf{g}^k = \frac{1}{2}\,(\bar{\mathbf{g}}_i \cdot \bar{\mathbf{g}}_k - \mathbf{g}_i \cdot \mathbf{g}_k)\,\mathbf{g}^i \otimes \mathbf{g}^k\,. \tag{7}$$

With the relation $\mathbf{E}_{\mathcal{B}} = \mathbf{Z}^{T-1}\mathbf{E}\,\bar{\mathbf{Z}}^{-1}$ the associated Green–Lagrangian strain tensor on the shell mid–surface is given by

$$\mathbf{E} = E_{ik}\,\mathbf{a}^i \otimes \mathbf{a}^k = \frac{1}{2}\,(\bar{\mathbf{g}}_i \cdot \bar{\mathbf{g}}_k - \mathbf{g}_i \cdot \mathbf{g}_k)\,\mathbf{a}^i \otimes \mathbf{a}^k\,. \tag{8}$$

Up to now basic equations of a standard approach for a shell formulation are derived. For a detailed discussion we refer to standard text books on shell theories.

Analyzing eq. (8) shows that we have to specify the base vectors in the reference and the current configuration which can be done using eqs. (2). Furthermore we introduce explicitly the base vectors in $\bar{\mathcal{B}}$ from $\bar{\mathbf{p}} = \bar{\mathbf{x}} + \zeta\mathbf{d}$

$$\bar{\mathbf{g}}_\alpha = \bar{\mathbf{a}}_\alpha + \zeta\mathbf{d}_{,\alpha} \qquad \bar{\mathbf{g}}_3 = \mathbf{d}\,. \tag{9}$$

The next step in a classical approach for the derivation of a shell theory is the representation of the convected basis $\bar{\mathbf{g}}_\alpha = \bar{\mathbf{a}}_\alpha + \zeta\mathbf{d}_{,\alpha}$ in terms of the base vectors of the reference configuration and the displacement vector $\mathbf{u} = u^\alpha\mathbf{a}_\alpha + u^3\mathbf{a}_3$ (this means a description of $\mathbf{u}$ with respect to the convected basis). It holds

$$\bar{\mathbf{g}}_\alpha = \bar{\mathbf{a}}_\alpha + \zeta\mathbf{d}_{,\alpha} = (\mathbf{a}_\alpha + \mathbf{u}_{,\alpha}) + \zeta(\mathbf{a}_{3,\alpha} + \mathbf{w}_{,\alpha})\,, \tag{10}$$

with the vector $\mathbf{w} = \mathbf{d} - \mathbf{a}_3$, see e.g. [PIE77]. For the further derivation of a shell formulation the gradients $\mathbf{u}_{,\alpha}$ and $\mathbf{w}_{,\alpha}$ have to be specified. Here a number of complicated terms occur due to the definitions of $\mathbf{u}$ and $\mathbf{w}$ with respect to $\mathbf{a}_i$. Especially for the last term approximations are used due to the degree of rotation which then restricts the applicability of the introduced shell formulation. Again we refer to standard textbooks on shell theories for a detailed discussion of this problem. Here we choose a different approach, where we will approximate the deformed base vectors $\bar{\mathbf{a}}_\alpha$ directly.

From (8) and (9) we obtain the components E_{ik} of the Green–Lagrangian strains on the shell mid–surface which leads to the following strain measures

$$\begin{aligned} \varepsilon_{\alpha\beta} &= 1/2(\bar{\mathbf{a}}_\alpha \cdot \bar{\mathbf{a}}_\beta - \mathbf{a}_\alpha \cdot \mathbf{a}_\beta) \\ \gamma_{\alpha 3} &= \bar{\mathbf{a}}_\alpha \cdot \mathbf{d} \\ \kappa_{\alpha\beta} &= 1/2(\bar{\mathbf{a}}_\alpha \cdot \mathbf{d}_{,\beta} + \bar{\mathbf{a}}_\beta \cdot \mathbf{d}_{,\alpha} - \mathbf{a}_\alpha \cdot \mathbf{a}_{3,\beta} - \mathbf{a}_\beta \cdot \mathbf{a}_{3,\alpha}) . \end{aligned} \tag{11}$$

Here $\varepsilon_{\alpha\beta}$ are the membrane strains, $\gamma_{\alpha 3}$ the shear strains and $\kappa_{\alpha\beta}$ the bending strains. Furthermore $\mathbf{a}_\alpha$, $\mathbf{a}_3$ and $\bar{\mathbf{a}}_\alpha$, $\mathbf{d}$ are the base vectors in the undeformed and deformed configurations, respectively. The indices α and β range from 1 to 2. The director vector $\mathbf{d}$ of the current configuration is obtained by an orthogonal transformation of the basis vector $\mathbf{t}_3$

$$\begin{aligned} \mathbf{d} &= \mathbf{R}\,\mathbf{t}_3 \\ \mathbf{R} &= \cos\varphi\,\mathbf{1} + \frac{\sin\varphi}{\varphi}\,\Omega + \frac{1-\cos\varphi}{\varphi^2}\,\theta\otimes\theta \end{aligned} \tag{12}$$

with the skew–symmetric tensor Ω defined by $\Omega\mathbf{a} = \theta \times \mathbf{a} \quad \forall \mathbf{a}$ and $\varphi = \|\theta\|$. This expression for $\mathbf{R} = \bar{\mathbf{t}}_i \otimes \mathbf{t}_i$ is the so–called Rodriguez formula.

There are a variety of possibilities to describe a rotation tensor, as e.g. Eulerian angles, Cardan angles, quaternions etc. A detailed survay may me found in [BUR92].

To describe the curvatures we need to compute the derivatives of $\mathbf{d}$ with respect to the coordinates Θ^α

$$\mathbf{d}_{,\alpha} = \mathbf{R}_{,\alpha}\,\mathbf{t}_3 + \mathbf{R}\,\mathbf{t}_{3,\alpha} . \tag{13}$$

Inserting $\mathbf{t}_3 = \mathbf{R}^T\mathbf{d}$ and $\mathbf{t}_3 = \mathbf{R}_0\,\mathbf{e}_3$ yields

$$\begin{aligned} \mathbf{d}_{,\alpha} &= \mathbf{R}_{,\alpha}\,\mathbf{R}^T\mathbf{d} + \mathbf{R}\mathbf{R}_{0,\alpha}\,\mathbf{R}_0^T\mathbf{R}^T\mathbf{d} \\ &= \bar{\theta}_\alpha \times \mathbf{d} \end{aligned} \tag{14}$$

where $\bar{\theta}_\alpha = \theta_\alpha + \mathbf{R}\theta_{0\alpha}$ and $\mathbf{R}_{0,\alpha}\,\mathbf{R}_0^T\,\mathbf{a} = \theta_{0\alpha} \times \mathbf{a} \quad \forall \mathbf{a}$. The derivative of $\mathbf{R}$ follows from (12)

$$\begin{aligned} \mathbf{R}_{,\alpha} = {} & [\,-\sin\varphi\,\mathbf{1} + \frac{\varphi\cos\varphi - \sin\varphi}{\varphi^2}\,\Omega \\ & + \frac{1}{\varphi^4}(\sin\varphi\varphi^2 - 2\varphi(1-\cos\varphi))\,\theta\otimes\theta\,]\;\varphi_{,\alpha} \\ & + \frac{\sin\varphi}{\varphi}\,\Omega_{,\alpha} + \frac{1-\cos\varphi}{\varphi^2}\,(\theta_{,\alpha}\otimes\theta + \theta\otimes\theta_{,\alpha}) \end{aligned} \tag{15}$$

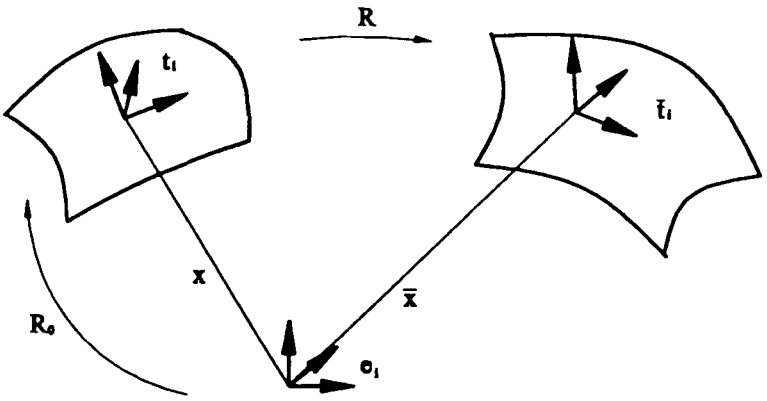

Figure 2: *Orthogonal transformation of the base systems*

with $\varphi_{,\alpha} = \theta \cdot \theta_{,\alpha} / \varphi$. After some algebra one obtains the axial vector $\theta_\alpha = \mathbf{H}\,\theta_{,\alpha}$, see [SIM90]

$$\mathbf{H} = \frac{\sin\varphi}{\varphi}\,\mathbf{1} + \left(\frac{1}{\varphi^2} - \frac{\sin\varphi}{\varphi^3}\right)\theta \otimes \theta + \frac{1-\cos\varphi}{\varphi^2}\Omega\,. \tag{16}$$

Remark 1:

1. According to standard shell theories all terms associated with ζ^2 are neglected. This assumption is valid for thin shells.
2. It occurs no shear flexure term which is consistent to the introduced kinematic assumption. $(\mathbf{d}_{,\alpha} \cdot \mathbf{d} = 0)$.
3. The construction of $\mathbf{a}_3$ leads to an unit normal vector. The director vector $\mathbf{d}$ is obtained by a rotation of $\mathbf{a}_3$. Thus $\mathbf{d}$ is an unit vector and within this theory no change of thickness h is described.

3 Stresses and Material Law

In this section we discuss the chosen material law. Here we use a layerwise description of the material behaviour which is valid for composite materials. We assume a purely elastic behaviour without damage or crack effects. Then the material law for the composite material bases on a linear relation between the 2^{nd}–Piola–Kirchoff stresses $\boldsymbol{\sigma}, \boldsymbol{\tau}$ and the components of the Green–Lagrangian strain tensor, which is valid for small strains. A two dimensional material law

in the tangent plane is then formulated for a layer k ($1 \leq k \leq NLAY$), where NLAY is the total number of layers, from

$$\boldsymbol{\sigma}^k = \mathbf{C}_G^k \left[\boldsymbol{\varepsilon} + \zeta^k \boldsymbol{\kappa}\right], \quad \boldsymbol{\tau}^k = \tilde{\mathbf{C}}_G^k \boldsymbol{\gamma}. \tag{17}$$

Here the main components of the stress and strain tensors are summarized in vectors ($\boldsymbol{\sigma} = [\sigma^{11}, \sigma^{22}, \sigma^{12}]^T, \boldsymbol{\tau} = [\tau^{13}, \tau^{13}]^T, \boldsymbol{\varepsilon} = [\varepsilon_{11}, \varepsilon_{22}, 2\varepsilon_{12}]^T, \boldsymbol{\kappa} = [\kappa_{11}, \kappa_{22}, 2\kappa_{12}]^T, \boldsymbol{\gamma} = [\gamma_{13}, \gamma_{13}]^T$). Stresses and strains are given in global directions. ζ^k describes the coordinate in thickness direction of the shell. The matrices $\mathbf{C}_G^k$ and $\tilde{\mathbf{C}}_G^k$ are calculated from the transformation of the locally defined orthotropic material matrices for shell like structures with the elasticity matrices

$$\mathbf{C}_L^k = \begin{bmatrix} C_{11} & C_{12} & 0 \\ C_{12} & C_{22} & 0 \\ 0 & 0 & C_{33} \end{bmatrix}_L, \quad \tilde{\mathbf{C}}_L^k = \begin{bmatrix} \tilde{C}_{11} & 0 \\ 0 & \tilde{C}_{22} \end{bmatrix}_L \tag{18}$$

in the globally introduced coordinate system. The transformation in the tangent plane from a local (x_{1L}, x_{2L}) coordinate system to a global (x_{1G}, x_{2G}) coordinate system is given by

$$\begin{bmatrix} x_{1L} \\ x_{2L} \end{bmatrix} = \begin{bmatrix} cos\varphi & sin\varphi \\ -sin\varphi & cos\varphi \end{bmatrix} \cdot \begin{bmatrix} x_{1G} \\ x_{2G} \end{bmatrix} \qquad \mathbf{x}_L = \mathbf{T}_x \mathbf{x}_G \tag{19}$$

with the rotation angle φ. Applying the chain rule we obtain the strains

$$\varepsilon_{11L} = \frac{\partial u_{1L}}{\partial x_{1L}} = \frac{\partial u_{1L}}{\partial x_{1G}} \cdot \frac{\partial x_{1G}}{\partial x_{1L}} + \frac{\partial u_{1L}}{\partial x_{2G}} \cdot \frac{\partial x_{2G}}{\partial x_{1L}}. \tag{20}$$

Introducing (19)

$$\begin{aligned} u_{1L} &= cos\varphi\, u_{1G} + sin\varphi\, u_{2G} \quad \text{in} \quad \frac{\partial u_{1L}}{\partial x_{1G}} \\ x_{1G} &= cos\varphi\, x_{1L} - sin\varphi\, x_{2L} \quad \text{in} \quad \frac{\partial x_{1G}}{\partial x_{1L}} \end{aligned} \tag{21}$$

leads to the result

$$\varepsilon_{11L} = cos^2\varphi\, \varepsilon_{11G} + sin^2\varphi\, \varepsilon_{22G} + sin\varphi\, cos\varphi\, \varepsilon_{12G}. \tag{22}$$

Thus the following relation can be derived

$$\boldsymbol{\varepsilon}_L = \mathbf{T}_\varepsilon\, \boldsymbol{\varepsilon}_G \tag{23}$$

$$\text{with} \qquad \mathbf{T}_\varepsilon = \begin{bmatrix} c^2 & s^2 & sc \\ s^2 & c^2 & -sc \\ -2sc & 2sc & c^2 - s^2 \end{bmatrix} \qquad \begin{matrix} s = sin\,\varphi \\ c = cos\,\varphi \end{matrix}. \tag{24}$$

A comparison of the specific internal energy

$$dW = \frac{1}{2}\boldsymbol{\sigma}_L^T \boldsymbol{\varepsilon}_L = \frac{1}{2}\boldsymbol{\sigma}_G^T \boldsymbol{\varepsilon}_G \tag{25}$$

yields the transformation for the stresses

$$\boldsymbol{\sigma}_L = \mathbf{T}_\sigma \boldsymbol{\sigma}_G \quad \text{with} \quad \mathbf{T}_\sigma = \mathbf{T}_\varepsilon^{T-1}, \tag{26}$$

and finally the relation for the material law

$$\boldsymbol{\sigma}_G = \mathbf{C}_G \boldsymbol{\varepsilon}_G \qquad \boldsymbol{\sigma}_L = \mathbf{C}_L \boldsymbol{\varepsilon}_L \quad \text{with} \qquad \mathbf{C}_G = \mathbf{T}_\varepsilon^T \mathbf{C}_L \mathbf{T}_\varepsilon . \tag{27}$$

This transformation is valid for the membrane strains $\boldsymbol{\varepsilon}$ and the bending strains $\boldsymbol{\kappa}$.

The transformation of the shear stresses and shear strains has to be carried out in a similar way. With $\mathbf{T}_\gamma = \mathbf{T}_\tau$ it holds

$$\tilde{\mathbf{C}}_G = \mathbf{T}_\tau^T \tilde{\mathbf{C}}_L \mathbf{T}_\tau . \tag{28}$$

After introducing this relation the following global material parameter occur

$$\begin{aligned}
C_{11G} &= c^4 C_{11L} + 2s^2c^2(C_{12L} + 2C_{33L}) + s^4 C_{22L} \\
C_{22G} &= s^4 C_{11L} + 2s^2c^2(C_{12L} + 2C_{33L}) + c^4 C_{22L} \\
C_{12G} &= s^2c^2(C_{11L} + C_{22L} - 4C_{33L}) + (s^4 + c^4)C_{12L} \\
C_{13G} &= c^3 s(C_{11L} - C_{12L} - 2C_{33L}) + s^3 c(C_{12L} - C_{22L} + 2C_{33L}) \\
C_{23G} &= s^3 c(C_{11L} - C_{12L} - 2C_{33L}) + c^3 s(C_{12L} - C_{22L} + 2C_{33L}) \\
C_{33G} &= s^2c^2(C_{11L} + C_{22L} - 2C_{12L} - 2C_{33L}) + (s^4 + c^4)C_{33L}
\end{aligned} \tag{29}$$

$$\begin{aligned}
\tilde{C}_{11G} &= c^2 \tilde{C}_{11L} + s^2 \tilde{C}_{22L} \\
\tilde{C}_{22G} &= s^2 \tilde{C}_{11L} + c^2 \tilde{C}_{22L} \\
\tilde{C}_{12G} &= sc(\tilde{C}_{11L} - \tilde{C}_{22L}) .
\end{aligned}$$

Within the transformation the symmetry of the material matrix is preserved, but the matrices are now fully populated.

A detailed derivation of these relations can be found in e.g. [TSA88].

The elements of the material matrices of a layer k depend on the elastic modules E_i of a three-dimensional material law in the following way, see e.g. [TSA88],

$$\begin{aligned}
C_{11L} &= \frac{1}{(1 - \nu^2 E_2/E_1)} E_1 \\
C_{22L} &= \frac{1}{(1 - \nu^2 E_2/E_1)} E_2 \\
C_{12L} &= \frac{1}{(1 - \nu^2 E_2/E_1)} E_2 \nu \\
C_{33L} &= C_{11L} = G_{12} \\
\tilde{C}_{22L} &= G_{23} .
\end{aligned} \tag{30}$$

Axis 1 is parallel to the fibers of the considered layer, while axis 2 is normal to the fiber direction.

The shell stress resultants and stress couples are introduced in a common way. The components of the associated tensors

$$\begin{aligned} N^{\alpha\beta} &= \int_{(h)} \sigma^{\alpha\beta} \det \mathbf{Z}\, d\zeta\,, \\ M^{\alpha\beta} &= \int_{(h)} \zeta\, \sigma^{\alpha\beta} \det \mathbf{Z}\, d\zeta\,, \\ Q^{\alpha 3} &= \int_{(h)} \kappa\, \tau^{\alpha 3} \det \mathbf{Z}\, d\zeta \end{aligned} \tag{31}$$

are summarized in the vectors $\mathbf{N} = [N^{11}, N^{22}, N^{12}]^T$, $\mathbf{M} = [M^{11}, M^{22}, M^{12}]^T$, $\mathbf{Q} = [Q^{13}, Q^{23}]^T$. Here, κ is the shear correction factor usually chosen as 5/6. Usually the determinant of the shifter tensor

$$\det \mathbf{Z} = \det(\mathbf{1} - \zeta \mathbf{B}) = 1 - \zeta\,(B_1^1 + B_2^2) + \zeta^2\,(B_1^1 B_2^2 - B_1^2 B_2^1) \tag{32}$$

is approximated by the first term which is valid for thin shells. Within the material law for these averaged global stresses we have the well known coupling effect between membrane and bending terms

$$\begin{bmatrix} \mathbf{N} \\ \mathbf{M} \\ \mathbf{Q} \end{bmatrix} = \begin{bmatrix} \mathbf{D}^m & \mathbf{D}^{mb} & \mathbf{0} \\ \mathbf{D}^{mbT} & \mathbf{D}^b & \mathbf{0} \\ \mathbf{0} & \mathbf{0} & \mathbf{D}^s \end{bmatrix} \cdot \begin{bmatrix} \boldsymbol{\varepsilon} \\ \boldsymbol{\kappa} \\ \boldsymbol{\gamma} \end{bmatrix} \tag{33}$$

with

$$\begin{aligned} \mathbf{D}^m &= \sum_{k=1}^{NLAY} \mathbf{C}^k\, h^k \\ \mathbf{D}^b &= \sum_{k=1}^{NLAY} \mathbf{C}^k \left[\frac{h^{k^3}}{12} h^k\, {\zeta_s^k}^2\right] \\ \mathbf{D}^{mb} &= \sum_{k=1}^{NLAY} \mathbf{C}^k\, h^k\, \zeta_s^k \\ \mathbf{D}^s &= \sum_{k=1}^{NLAY} \tilde{\mathbf{C}}^k\, h^k \end{aligned} \tag{34}$$

In (34) h^k is the thickness of the k-th layer, ζ_s^k is the distance from the midpoint of the considered layer to the reference surface and $NLAY$ is the total number of layers.

4 Weak Form – Principle of Virtual Work

The numerical treatment within the finite element method is based on the principle of virtual work. It is given with reference to the undeformed shell

configuration in a Lagrangian description by

$$D\pi \cdot \delta \mathbf{v} = \int_{\Omega} [\mathbf{N} \cdot \delta \boldsymbol{\varepsilon} + \mathbf{M} \cdot \delta \boldsymbol{\kappa} + \mathbf{Q} \cdot \delta \boldsymbol{\gamma}]\, d\Omega - \int_{\Omega_\sigma} \hat{\mathbf{t}} \cdot \delta \mathbf{v}\, d\Omega = 0. \qquad (35)$$

In eq. (35) π is the potential energy calculated in the domain Ω, the first r.h.s. term describes the virtual work of the internal forces while the last term describes the virtual work of the external forces, given in a simplified formulation.

Thus we have to specify the variations of the shell strains $\delta\boldsymbol{\varepsilon} = [\delta\varepsilon_{11}, \delta\varepsilon_{22}, 2\delta\varepsilon_{12}]^T$, $\delta\boldsymbol{\kappa} = [\delta\kappa_{11}, \delta\kappa_{22}, 2\delta\kappa_{12}]^T$, $\delta\boldsymbol{\gamma} = [\delta\gamma_{13}, \delta\gamma_{13}]^T$. Using (11) one obtains

$$\begin{aligned} \delta\varepsilon_{\alpha\beta} &= \tfrac{1}{2}(\delta\bar{\mathbf{a}}_\alpha \cdot \bar{\mathbf{a}}_\beta + \bar{\mathbf{a}}_\alpha \cdot \delta\bar{\mathbf{a}}_\beta) \\ \delta\gamma_{\alpha 3} &= \delta\bar{\mathbf{a}}_\alpha \cdot \mathbf{d} + \bar{\mathbf{a}}_\alpha \cdot \delta\mathbf{d} \\ \delta\kappa_{\alpha\beta} &= \tfrac{1}{2}(\delta\bar{\mathbf{a}}_\alpha \cdot \mathbf{d}_{,\beta} + \delta\bar{\mathbf{a}}_\beta \cdot \mathbf{d}_{,\alpha} + \bar{\mathbf{a}}_\alpha \cdot \delta\mathbf{d}_{,\beta} + \bar{\mathbf{a}}_\beta \cdot \delta\mathbf{d}_{,\alpha}) \end{aligned} \qquad (36)$$

In (36) $\delta\mathbf{d}$ and $\delta\mathbf{d}_{,\beta}$ are to be derived. The variation of $\mathbf{d}$ follows from (12)

$$\delta\mathbf{d} = \delta\mathbf{R}\,\mathbf{t}_3 = \delta\boldsymbol{\Omega}\mathbf{d} = \delta\boldsymbol{\theta} \times \mathbf{d} \qquad (37)$$

where $\delta\boldsymbol{\theta}$ denotes the axial vector of the skew-symmetric tensor $\delta\boldsymbol{\Omega} = \delta\mathbf{R}\mathbf{R}^T$. The director vector $\mathbf{d}$ is orthogonal to $\bar{\mathbf{t}}_1$ and $\bar{\mathbf{t}}_2$, thus $\mathbf{d} = \bar{\mathbf{t}}_1 \times \bar{\mathbf{t}}_2$. Hence we may rewrite (37) as

$$\delta\mathbf{d} = \mathbf{W}_3\, \delta\boldsymbol{\theta} \qquad (38)$$

with $\mathbf{W}_3 = -\mathbf{W}_3^T = \bar{\mathbf{t}}_1 \otimes \bar{\mathbf{t}}_2 - \bar{\mathbf{t}}_2 \otimes \bar{\mathbf{t}}_1$. Furthermore using (37) we obtain

$$\delta\mathbf{d}_{,\beta} = \delta\boldsymbol{\theta}_{,\beta} \times \mathbf{d} + \delta\boldsymbol{\theta} \times \mathbf{d}_{,\beta} \qquad (39)$$

and

$$\begin{aligned} \bar{\mathbf{a}}_\alpha \cdot \delta\mathbf{d}_{,\beta} &= \bar{\mathbf{a}}_\alpha \cdot (\delta\boldsymbol{\theta}_{,\beta} \times \mathbf{d}) + \bar{\mathbf{a}}_\alpha \cdot (\delta\boldsymbol{\theta} \times \mathbf{d}_{,\beta}) \\ &= (\mathbf{d} \times \bar{\mathbf{a}}_\alpha) \cdot \delta\boldsymbol{\theta}_{,\beta} + (\mathbf{d}_{,\beta} \times \bar{\mathbf{a}}_\alpha) \cdot \delta\boldsymbol{\theta}. \end{aligned} \qquad (40)$$

The geometrical nonlinear load deflection behaviour is calculated with a Newton-type iteration procedure. For this purpose we need to derive the linearization of the principle of virtual work

$$\begin{aligned} D[D\pi \cdot \delta\mathbf{v}] \cdot \Delta\mathbf{v} \quad = \quad & \int_{\Omega} \delta\boldsymbol{\varepsilon} \cdot \mathbf{D}^m \Delta\boldsymbol{\varepsilon}\, d\Omega + \int_{\Omega} \delta\boldsymbol{\varepsilon} \cdot \mathbf{D}^{mb} \Delta\boldsymbol{\kappa}\, d\Omega \\ + & \int_{\Omega} \delta\boldsymbol{\kappa} \cdot \mathbf{D}^{mbT} \Delta\boldsymbol{\varepsilon}\, d\Omega + \int_{\Omega} \delta\boldsymbol{\kappa} \cdot \mathbf{D}^{b} \Delta\boldsymbol{\kappa}\, d\Omega \\ + & \int_{\Omega} \delta\boldsymbol{\gamma} \cdot \mathbf{D}^{s} \Delta\boldsymbol{\gamma}\, d\Omega + \int_{\Omega} \Delta\delta\boldsymbol{\varepsilon} \cdot \mathbf{N}\, d\Omega \\ + & \int_{\Omega} \Delta\delta\boldsymbol{\kappa} \cdot \mathbf{M}\, d\Omega + \int_{\Omega} \Delta\delta\boldsymbol{\gamma} \cdot \mathbf{Q}\, d\Omega. \end{aligned} \qquad (41)$$

Here the linearized shell strains are defined as $\Delta\boldsymbol{\varepsilon} = [\Delta\varepsilon_{11}, \Delta\varepsilon_{22}, 2\Delta\varepsilon_{12}]^T$, $\Delta\boldsymbol{\kappa} = [\Delta\kappa_{11}, \Delta\kappa_{22}, 2\Delta\kappa_{12}]^T$ and $\Delta\boldsymbol{\gamma} = [\Delta\gamma_{13}, \Delta\gamma_{13}]^T$. The operator δ in (36) simply has to be replaced by Δ.

The linearization of the virtual strains yields $\Delta\delta\boldsymbol{\varepsilon} = [\Delta\delta\varepsilon_{11}, \Delta\delta\varepsilon_{22}, 2\Delta\delta\varepsilon_{12}]^T$, $\Delta\delta\boldsymbol{\kappa} = [\Delta\delta\kappa_{11}, \Delta\delta\kappa_{22}, 2\Delta\delta\kappa_{12}]^T$ and $\Delta\delta\boldsymbol{\gamma} = [\Delta\delta\gamma_{13}, \Delta\delta\gamma_{13}]^T$ with

$$\begin{aligned}
\Delta\delta\varepsilon_{\alpha\beta} &= \tfrac{1}{2}(\,\delta\bar{\mathbf{a}}_\alpha \cdot \Delta\bar{\mathbf{a}}_\beta + \Delta\bar{\mathbf{a}}_\alpha \cdot \delta\bar{\mathbf{a}}_\beta) \\
\Delta\delta\gamma_{\alpha 3} &= \delta\bar{\mathbf{a}}_\alpha \cdot \Delta\mathbf{d} + \Delta\bar{\mathbf{a}}_\alpha \cdot \delta\mathbf{d} + \bar{\mathbf{a}}_\alpha \cdot \Delta\delta\mathbf{d} \\
\Delta\delta\kappa_{\alpha\beta} &= \tfrac{1}{2}\;(\delta\bar{\mathbf{a}}_\alpha \cdot \Delta\mathbf{d}_{,\beta} + \delta\bar{\mathbf{a}}_\beta \cdot \Delta\mathbf{d}_{,\alpha} + \Delta\bar{\mathbf{a}}_\alpha \cdot \delta\mathbf{d}_{,\beta} + \Delta\bar{\mathbf{a}}_\beta \cdot \delta\mathbf{d}_{,\alpha} \\
&\qquad + \bar{\mathbf{a}}_\alpha \cdot \Delta\delta\mathbf{d}_{,\beta} + \bar{\mathbf{a}}_\beta \cdot \Delta\delta\mathbf{d}_{,\alpha})\,.
\end{aligned} \tag{42}$$

The second variation $\Delta\delta\mathbf{d}$ follows from

$$\begin{aligned}
\Delta\delta\mathbf{d} &= \delta\boldsymbol{\theta} \times (\Delta\boldsymbol{\theta} \times \mathbf{d}) \\
&= \Delta\boldsymbol{\theta}\,(\delta\boldsymbol{\theta} \cdot \mathbf{d}) - \mathbf{d}(\delta\boldsymbol{\theta} \cdot \Delta\boldsymbol{\theta}) \\
\bar{\mathbf{a}}_\alpha \cdot \Delta\delta\mathbf{d} &= (\bar{\mathbf{a}}_\alpha \cdot \Delta\boldsymbol{\theta})(\delta\boldsymbol{\theta} \cdot \mathbf{d}) - (\bar{\mathbf{a}}_\alpha \cdot \mathbf{d})(\delta\boldsymbol{\theta} \cdot \Delta\boldsymbol{\theta}) \\
&= \delta\boldsymbol{\theta} \cdot \mathbf{A}_\alpha\,\Delta\boldsymbol{\theta}
\end{aligned} \tag{43}$$

where $\mathbf{A}_\alpha = \frac{1}{2}(\mathbf{d} \otimes \bar{\mathbf{a}}_\alpha + \bar{\mathbf{a}}_\alpha \otimes \mathbf{d}) - (\bar{\mathbf{a}}_\alpha \cdot \mathbf{d})\mathbf{1}$.

The expression $\delta\bar{\mathbf{a}}_\alpha \cdot \Delta\mathbf{d}_{,\beta}$ is given by

$$\begin{aligned}
\delta\bar{\mathbf{a}}_\alpha \cdot \Delta\mathbf{d}_{,\beta} &= \delta\bar{\mathbf{a}}_\alpha \cdot\; [\Delta\boldsymbol{\theta}_{,\beta} \times \mathbf{d} + \Delta\boldsymbol{\theta} \times \mathbf{d}_{,\beta}] \\
&= \delta\bar{\mathbf{a}}_\alpha \cdot\; [\Delta\boldsymbol{\theta}_{,\beta} \times (\bar{\mathbf{t}}_1 \times \bar{\mathbf{t}}_2) + \Delta\boldsymbol{\theta} \times (\bar{\boldsymbol{\theta}}_\beta \times \mathbf{d})] \\
&= \delta\bar{\mathbf{a}}_\alpha \cdot\; [\mathbf{W}_3\Delta\boldsymbol{\theta}_{,\beta} + \mathbf{W}_\beta\Delta\boldsymbol{\theta}\;]\quad .
\end{aligned} \tag{44}$$

with $\mathbf{W}_\beta = \bar{\boldsymbol{\theta}}_\beta \otimes \mathbf{d} - \mathbf{d} \otimes \bar{\boldsymbol{\theta}}_\beta$. Inserting

$$\begin{aligned}
\Delta\delta\mathbf{d}_{,\beta} &= \delta\boldsymbol{\theta}_{,\beta} \times \Delta\mathbf{d} + \delta\boldsymbol{\theta} \times \Delta\mathbf{d}_{,\beta} \\
&= \delta\boldsymbol{\theta}_{,\beta} \times (\Delta\boldsymbol{\theta} \times \mathbf{d}) + \delta\boldsymbol{\theta} \times (\Delta\boldsymbol{\theta}_{,\beta} \times \mathbf{d}) + \delta\boldsymbol{\theta} \times (\Delta\boldsymbol{\theta} \times \mathbf{d}_{,\beta}) \\
&= \Delta\boldsymbol{\theta}(\delta\boldsymbol{\theta}_{,\beta} \cdot \mathbf{d}) - \mathbf{d}(\delta\boldsymbol{\theta}_{,\beta} \cdot \Delta\boldsymbol{\theta}) + \Delta\boldsymbol{\theta}_{,\beta}\,(\delta\boldsymbol{\theta} \cdot \mathbf{d}) - \mathbf{d}(\delta\boldsymbol{\theta} \cdot \Delta\boldsymbol{\theta}_{,\beta}) \\
&\quad + \Delta\boldsymbol{\theta}(\delta\boldsymbol{\theta} \cdot \mathbf{d}_{,\beta}) - \mathbf{d}(\delta\boldsymbol{\theta} \cdot \Delta\boldsymbol{\theta})
\end{aligned} \tag{45}$$

into $\bar{\mathbf{a}}_\alpha \cdot \Delta\delta\mathbf{d}_{,\beta}$ yields

$$\begin{aligned}
\bar{\mathbf{a}}_\alpha \cdot \Delta\delta\mathbf{d}_{,\beta} &= (\bar{\mathbf{a}}_\alpha \cdot \Delta\boldsymbol{\theta})(\delta\boldsymbol{\theta}_{,\beta} \cdot \mathbf{d}) - (\bar{\mathbf{a}}_\alpha \cdot \mathbf{d})(\delta\boldsymbol{\theta}_{,\beta} \cdot \Delta\boldsymbol{\theta}) \\
&\quad + (\bar{\mathbf{a}}_\alpha \cdot \Delta\boldsymbol{\theta}_{,\beta})(\delta\boldsymbol{\theta} \cdot \mathbf{d}) - (\bar{\mathbf{a}}_\alpha \cdot \mathbf{d})(\delta\boldsymbol{\theta} \cdot \Delta\boldsymbol{\theta}_{,\beta}) \\
&\quad + (\bar{\mathbf{a}}_\alpha \cdot \Delta\boldsymbol{\theta})(\delta\boldsymbol{\theta} \cdot \mathbf{d}_{,\beta}) - (\bar{\mathbf{a}}_\alpha \cdot \mathbf{d}_{,\beta})(\delta\boldsymbol{\theta} \cdot \Delta\boldsymbol{\theta})\quad .
\end{aligned} \tag{46}$$

Thus one can rewrite (42) as

$$
\begin{aligned}
\Delta\delta\varepsilon_{\alpha\beta} &= \tfrac{1}{2}(\,\delta\bar{\mathbf{a}}_\alpha\cdot\mathbf{1}\Delta\bar{\mathbf{a}}_\beta+\Delta\bar{\mathbf{a}}_\alpha\cdot\mathbf{1}\delta\bar{\mathbf{a}}_\beta\,)\\
\Delta\delta\gamma_{\alpha 3} &= \delta\bar{\mathbf{a}}_\alpha\cdot\mathbf{W}_3\Delta\boldsymbol{\theta}+\Delta\bar{\mathbf{a}}_\alpha\cdot\mathbf{W}_3\delta\boldsymbol{\theta}+\delta\boldsymbol{\theta}\cdot\mathbf{A}_\alpha\Delta\boldsymbol{\theta}\\
\Delta\delta\kappa_{\alpha\beta} &= \tfrac{1}{2}[\;\delta\bar{\mathbf{a}}_\alpha\cdot(\mathbf{W}_3\Delta\boldsymbol{\theta}_{,\beta}+\mathbf{W}_\beta\Delta\boldsymbol{\theta})\\
&\quad+\delta\bar{\mathbf{a}}_\beta\cdot(\mathbf{W}_3\Delta\boldsymbol{\theta}_{,\alpha}+\mathbf{W}_\alpha\Delta\boldsymbol{\theta})\\
&\quad+(\delta\boldsymbol{\theta}_{,\beta}\,\mathbf{W}_3^T+\delta\boldsymbol{\theta}\mathbf{W}_\beta^T)\cdot\Delta\bar{\mathbf{a}}_\alpha\\
&\quad+(\delta\boldsymbol{\theta}_{,\alpha}\,\mathbf{W}_3^T+\delta\boldsymbol{\theta}\mathbf{W}_\alpha^T)\cdot\Delta\bar{\mathbf{a}}_\beta\\
&\quad+\delta\boldsymbol{\theta}_{,\beta}\cdot\mathbf{A}_\alpha\Delta\boldsymbol{\theta}+\delta\boldsymbol{\theta}\cdot\mathbf{A}_\alpha\Delta\boldsymbol{\theta}_{,\beta}+\delta\boldsymbol{\theta}\cdot\mathbf{A}_{\alpha\beta}\Delta\boldsymbol{\theta}\\
&\quad+\delta\boldsymbol{\theta}_{,\alpha}\cdot\mathbf{A}_\beta\Delta\boldsymbol{\theta}+\delta\boldsymbol{\theta}\cdot\mathbf{A}_\beta\Delta\boldsymbol{\theta}_{,\alpha}+\delta\boldsymbol{\theta}\cdot\mathbf{A}_{\beta\alpha}\Delta\boldsymbol{\theta}\;]\,.
\end{aligned}
\tag{47}
$$

Here we use the abbreviation $\mathbf{A}_{\alpha\beta}=\frac{1}{2}\left(\mathbf{d}_{,\beta}\otimes\bar{\mathbf{a}}_\alpha+\bar{\mathbf{a}}_\alpha\otimes\mathbf{d}_{,\beta}\right)-\left(\bar{\mathbf{a}}_\alpha\cdot\mathbf{d}_{,\beta}\right)\mathbf{1}$.

Remark 2:

1. The given formulation is completely nonlinear. Thus no discussion is necessary which terms have to be used and which not as in classical geometrical nonlinear shell theories, see e.g. [PIE77].
2. There is no simplification in the description of the director vector and its derivations.
3. With the introduced director vector it is possible to describe rotations without limitations.
4. The complete nonlinear formulation is essential in the deep nonlinear range.

5 Finite Element Formulation

In this section we will discuss briefly the formulation of the associated finite element. We introduce a general finite element discretization

$$
B^h=\bigcup_{e=1}^{n_{elm}}\Omega_e \tag{48}
$$

with n_{elm} elements. The formulation is based on the isoparametric concept. Within an element Ω_e the position vector $\mathbf{x}$ of the initial configuration is approximated by

$$
\mathbf{x}^h \;=\; x_i\,\mathbf{e}_i \;=\; \sum_{I=1}^{nel} N_I\mathbf{x}_I\,. \tag{49}
$$

Here N_I and $\mathbf{x}_I$ are the shape functions and the vector of nodal coordinates, respectively. We use as shape functions N_I Lagrange- or Serendipity shape

functions. Furthermore *nel* defines the total number of nodes at the element. For quadrilaterals it holds

$$N_I(\xi,\eta) = \frac{1}{4}(1+\xi\,\xi_I)(1+\eta\,\eta_I)\,. \tag{50}$$

Using (49) the undeformed basis $\mathbf{a}_\xi$, $\mathbf{a}_\eta$ and $\mathbf{a}_\zeta$ at the integration points can be expressed

$$\begin{aligned} \mathbf{a}_\xi &= \sum_{I=1}^{nel} N_{I,\xi}\,\mathbf{x}_I\,, \\ \mathbf{a}_\eta &= \sum_{I=1}^{nel} N_{I,\eta}\,\mathbf{x}_I\,, \\ \mathbf{a}_\zeta &= (\mathbf{a}_\xi \times \mathbf{a}_\eta)/\|\mathbf{a}_\xi \times \mathbf{a}_\eta\|\,. \end{aligned} \tag{51}$$

Next the initial rotation tensor $\mathbf{R}_0 = \mathbf{t}_i \otimes \mathbf{e}_i$ with basis vectors $\mathbf{t}_i$ can be expressed as follows

$$\begin{aligned} \mathbf{t}_1 &= \mathbf{a}_\xi/\|\mathbf{a}_\xi\|\,, \\ \mathbf{t}_3 &= \mathbf{a}_\zeta\,, \\ \mathbf{t}_2 &= \mathbf{a}_3 \times \mathbf{a}_1\,. \end{aligned} \tag{52}$$

Associated with this basis system are coordinates Θ_α. The shape function derivatives $\partial N_I/\partial\Theta_\alpha := N_{I,\alpha}$ can be obtained applying the chain rule to $\mathbf{x}$

$$\frac{\partial \mathbf{x}}{\partial \xi_\alpha} = \frac{\partial \mathbf{x}}{\partial \Theta_\beta}\frac{\partial \Theta_\beta}{\partial \xi_\alpha} \qquad \text{with } \xi_1 = \xi,\ \xi_2 = \eta\,. \tag{53}$$

With (51) and (52) we can introduce the base vectors $\mathbf{a}_{\xi_\alpha}$ by

$$\mathbf{a}_{\xi_\alpha} = \mathbf{t}_\beta \frac{\partial \Theta_\beta}{\partial \xi_\alpha} \tag{54}$$

which leads with $\mathbf{a}_{\xi_\alpha}\cdot\mathbf{t}_\beta = \dfrac{\partial\Theta_\beta}{\partial\xi_\alpha}$ to the components $J_{\alpha\beta}$ of the Jacobian matrix

$$\mathbf{J} = \begin{bmatrix} \mathbf{a}_\xi\cdot\mathbf{t}_1 & \mathbf{a}_\xi\cdot\mathbf{t}_2 \\ \mathbf{a}_\eta\cdot\mathbf{t}_1 & \mathbf{a}_\eta\cdot\mathbf{t}_2 \end{bmatrix}. \tag{55}$$

Thus the derivatives $\dfrac{\partial \mathbf{x}}{\partial \xi_\alpha}$ are defined by

$$\frac{\partial \mathbf{x}}{\partial \xi_\alpha} = J_{\alpha\beta}\frac{\partial \mathbf{x}}{\partial \Theta_\beta}\,. \tag{56}$$

This relation holds also for the shape functions N_I when considering (49). Thus the derivatives of N_I with respect to Θ_α are then expressed with the inverse relation

$$\begin{bmatrix} N_{I,1} \\ N_{I,2} \end{bmatrix} = \mathbf{J}^{-1}\begin{bmatrix} N_{I,\xi} \\ N_{I,\eta} \end{bmatrix}. \tag{57}$$

The current configuration is obtained by interpolating the displacement vector $\mathbf{u}$ and the rotation vector $\boldsymbol{\theta}$ within the element

$$\begin{aligned} \mathbf{u}^h &= u_i^h \mathbf{e}_i = \sum_{I=1}^{nel} N_I \mathbf{u}_I \\ \boldsymbol{\theta}^h &= \theta_i^h \mathbf{e}_i = \sum_{I=1}^{nel} N_I \boldsymbol{\theta}_I \,. \end{aligned} \tag{58}$$

Note that the components of both the displacement vector and the axial vector are introduced with respect to the Cartesian coordinate system.

With these preliminary interpolations at hand the deformed base vectors $\bar{\mathbf{a}}_\alpha$ and variations $\delta\bar{\mathbf{a}}_\alpha$ can be computed within the element domain

$$\begin{aligned} \bar{\mathbf{a}}_\alpha &= \bar{\mathbf{x}}_{,\alpha} = \sum_{I=1}^{nel} N_{I,\alpha} \left(\mathbf{x}_I + \mathbf{u}_I\right) \\ \delta\bar{\mathbf{a}}_\alpha &= \sum_{I=1}^{nel} N_{I,\alpha}\, \delta\mathbf{u}_I \,. \end{aligned} \tag{59}$$

To avoid shear locking the transverse shear strains are independently interpolated within the element, see e.g. [BAD85],[DVB84]. This seems to be up to now the best formulation for Reissner–Mindlin based plate and shell formulations. A similar procedure for 8- and 9-node elements is proposed in [PIJ87].

For this purpose the shear strains $\tilde{\gamma} = [\tilde{\gamma}_{\xi 3},\ \tilde{\gamma}_{\eta 3}]^T$ are interpolated using a constant–linear interpolation, see [BAD85], [DVB84]

$$\begin{bmatrix} \tilde{\gamma}_{\xi 3} \\ \tilde{\gamma}_{\eta 3} \end{bmatrix} = \frac{1}{2} \begin{bmatrix} (1-\eta)\gamma_{\xi 3B} + (1+\eta)\gamma_{\xi 3D} \\ (1-\xi)\gamma_{\eta 3A} + (1+\xi)\gamma_{\eta 3C} \end{bmatrix} . \tag{60}$$

Here

$$\begin{aligned} \gamma_{\eta 3A} &= \bar{\mathbf{a}}_{\eta A} \cdot \mathbf{d}_A \qquad & \gamma_{\eta 3C} &= \bar{\mathbf{a}}_{\eta C} \cdot \mathbf{d}_C \\ \gamma_{\xi 3B} &= \bar{\mathbf{a}}_{\xi B} \cdot \mathbf{d}_B \qquad & \gamma_{\xi 3D} &= \bar{\mathbf{a}}_{\xi D} \cdot \mathbf{d}_D \end{aligned} \tag{61}$$

are the transverse shear strains computed from the displacement field at the midside nodes $M = A, B, C, D$, as depicted in Figure 3.

The deformed tangential base vectors at the sampling points are given by

$$\begin{aligned} \bar{\mathbf{a}}_{\eta A} &= \tfrac{1}{2}(\bar{\mathbf{x}}_4 - \bar{\mathbf{x}}_1) \qquad & \bar{\mathbf{a}}_{\eta C} &= \tfrac{1}{2}(\bar{\mathbf{x}}_3 - \bar{\mathbf{x}}_2) \\ \bar{\mathbf{a}}_{\xi B} &= \tfrac{1}{2}(\bar{\mathbf{x}}_2 - \bar{\mathbf{x}}_1) \qquad & \bar{\mathbf{a}}_{\xi D} &= \tfrac{1}{2}(\bar{\mathbf{x}}_3 - \bar{\mathbf{x}}_4) \end{aligned} \tag{62}$$

and $\mathbf{d}_M = \mathbf{d}(\boldsymbol{\theta}_M)$ is obtained using (12) with

$$\begin{aligned} \boldsymbol{\theta}_A &= \tfrac{1}{2}(\boldsymbol{\theta}_4 + \boldsymbol{\theta}_1) \qquad & \boldsymbol{\theta}_C &= \tfrac{1}{2}(\boldsymbol{\theta}_2 + \boldsymbol{\theta}_3) \\ \boldsymbol{\theta}_B &= \tfrac{1}{2}(\boldsymbol{\theta}_1 + \boldsymbol{\theta}_2) \qquad & \boldsymbol{\theta}_D &= \tfrac{1}{2}(\boldsymbol{\theta}_3 + \boldsymbol{\theta}_4) \end{aligned} \tag{63}$$

The variation of the shear strains is given by

$$\begin{bmatrix} \delta\tilde{\gamma}_{\xi 3} \\ \delta\tilde{\gamma}_{\eta 3} \end{bmatrix} = \frac{1}{2} \begin{bmatrix} (1-\eta)\delta\gamma_{\xi 3B} + (1+\eta)\delta\gamma_{\xi 3D} \\ (1-\xi)\delta\gamma_{\eta 3A} + (1+\xi)\delta\gamma_{\eta 3C} \end{bmatrix} . \tag{64}$$

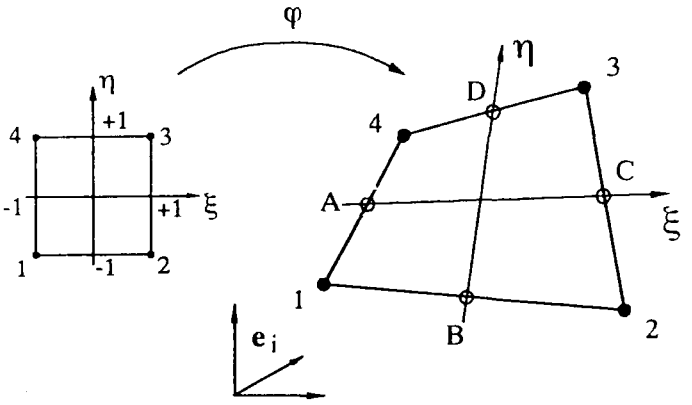

Figure 3: *Isoparametric 4-node element*

with

$$\begin{aligned} \delta\gamma_{\eta 3A} &= \delta\bar{\mathbf{a}}_{\eta A}\cdot\mathbf{d}_A + \bar{\mathbf{a}}_{\eta A}\cdot\delta\mathbf{d}_A \qquad \delta\gamma_{\eta 3C} = \delta\bar{\mathbf{a}}_{\eta C}\cdot\mathbf{d}_C + \bar{\mathbf{a}}_{\eta C}\cdot\delta\mathbf{d}_C \\ \delta\gamma_{\xi 3B} &= \delta\bar{\mathbf{a}}_{\xi B}\cdot\mathbf{d}_B + \bar{\mathbf{a}}_{\xi B}\cdot\delta\mathbf{d}_B \qquad \delta\gamma_{\xi 3D} = \delta\bar{\mathbf{a}}_{\xi D}\cdot\mathbf{d}_D + \bar{\mathbf{a}}_{\xi D}\cdot\delta\mathbf{d}_D \end{aligned} \tag{65}$$

and

$$\begin{aligned} \delta\bar{\mathbf{a}}_{\eta A} &= \tfrac{1}{2}(\delta\mathbf{u}_4 - \delta\mathbf{u}_1) \qquad \delta\bar{\mathbf{a}}_{\eta C} = \tfrac{1}{2}(\delta\mathbf{u}_3 - \delta\mathbf{u}_2) \\ \delta\bar{\mathbf{a}}_{\xi B} &= \tfrac{1}{2}(\delta\mathbf{u}_2 - \delta\mathbf{u}_1) \qquad \delta\bar{\mathbf{a}}_{\xi D} = \tfrac{1}{2}(\delta\mathbf{u}_3 - \delta\mathbf{u}_4) \end{aligned} \tag{66}$$

At the midside nodes one obtains with (63)

$$\begin{aligned} \delta\theta_A &= \tfrac{1}{2}(\delta\theta_4 + \delta\theta_1) \qquad \delta\theta_C = \tfrac{1}{2}(\delta\theta_2 + \delta\theta_3) \\ \delta\theta_B &= \tfrac{1}{2}(\delta\theta_1 + \delta\theta_2) \qquad \delta\theta_D = \tfrac{1}{2}(\delta\theta_3 + \delta\theta_4) \end{aligned} \tag{67}$$

The finite element formulation of the membrane part yields

$$\delta\boldsymbol{\varepsilon}^h = \sum_{I=1}^{nel} \mathbf{B}_I^m\,\delta\mathbf{v}_I \tag{68}$$

with matrix $\mathbf{B}_I^m$

$$\mathbf{B}_I^m = \begin{bmatrix} \bar{\mathbf{a}}_1^T N_{I,1} & 0 \\ \bar{\mathbf{a}}_2^T N_{I,2} & 0 \\ \bar{\mathbf{a}}_1^T N_{I,2} + \bar{\mathbf{a}}_2^T N_{I,1} & 0 \end{bmatrix} \tag{69}$$

and the virtual nodal displacement vector $\delta\mathbf{v}_I = [\delta\mathbf{u}_I, \delta\theta_I]^T$ of node I. The finite element formulation of the shear strains is expressed as

$$\delta\tilde{\boldsymbol{\gamma}}^h = \sum_{I=1}^{nel} \mathbf{B}_I^s\,\delta\mathbf{v}_I \tag{70}$$

with

$$\begin{aligned}
\mathbf{B}_1^s &= \begin{bmatrix} N_{1,\xi}\,\mathbf{d}_B^T & -N_{1,\xi}\,(\mathbf{d}_B \times \bar{\mathbf{a}}_{\xi B})^T \\ N_{1,\eta}\,\mathbf{d}_A^T & -N_{1,\eta}\,(\mathbf{d}_A \times \bar{\mathbf{a}}_{\eta A})^T \end{bmatrix} \\
\mathbf{B}_2^s &= \begin{bmatrix} N_{2,\xi}\,\mathbf{d}_B^T & N_{2,\xi}\,(\mathbf{d}_B \times \bar{\mathbf{a}}_{\xi B})^T \\ N_{2,\eta}\,\mathbf{d}_C^T & -N_{2,\eta}\,(\mathbf{d}_C \times \bar{\mathbf{a}}_{\xi C})^T \end{bmatrix} \\
\mathbf{B}_3^s &= \begin{bmatrix} N_{3,\xi}\,\mathbf{d}_D^T & N_{3,\xi}\,(\mathbf{d}_D \times \bar{\mathbf{a}}_{\eta D})^T \\ N_{3,\eta}\,\mathbf{d}_C^T & N_{3,\eta}\,(\mathbf{d}_C \times \bar{\mathbf{a}}_{\xi C})^T \end{bmatrix} \\
\mathbf{B}_4^s &= \begin{bmatrix} N_{4,\xi}\,\mathbf{d}_D^T & -N_{4,\xi}\,(\mathbf{d}_D \times \bar{\mathbf{a}}_{\eta D})^T \\ N_{4,\eta}\,\mathbf{d}_A^T & N_{4,\eta}\,(\mathbf{d}_A \times \bar{\mathbf{a}}_{\eta A})^T \end{bmatrix} .
\end{aligned} \tag{71}$$

The variation of the bending part is given by $(36)_3$. Based on these formulaes the approximation of the bending part follows from

$$\delta\boldsymbol{\kappa}^h = \sum_{I=1}^{nel} \mathbf{B}_I^b\, \delta\mathbf{v}_I \tag{72}$$

with

$$\mathbf{B}_I^b = \begin{bmatrix} N_{I,1}\,\mathbf{d}_{,1}^T & N_{I,1}\,(\mathbf{d} \times \bar{\mathbf{a}}_1)^T + N_I(\mathbf{d}_{,1} \times \bar{\mathbf{a}}_1)^T \\ N_{I,2}\,\mathbf{d}_{,2}^T & N_{I,2}\,(\mathbf{d} \times \bar{\mathbf{a}}_2)^T + N_I(\mathbf{d}_{,2} \times \bar{\mathbf{a}}_2)^T \\ N_{I,2}\,\mathbf{d}_{,1}^T & N_{I,1}\,(\mathbf{d} \times \bar{\mathbf{a}}_2)^T + N_I(\mathbf{d}_{,1} \times \bar{\mathbf{a}}_2)^T \\ +N_{I,1}\,\mathbf{d}_{,2}^T & N_{I,2}\,(\mathbf{d} \times \bar{\mathbf{a}}_1)^T + N_I(\mathbf{d}_{,2} \times \bar{\mathbf{a}}_1)^T \end{bmatrix} . \tag{73}$$

Based on this element specific formulation we define the residual (on element level) in a standard way for a nodal displacement vector

$$\begin{aligned}
G_e^h(\mathbf{v}_e, \delta\mathbf{v}_e) = \sum_{I=1}^{nel} \delta\mathbf{v}_I^T \{ & \int_{\Omega_e} \mathbf{B}_I^{mT}(\mathbf{v}_e)\mathbf{N}(\mathbf{v}_e) + \mathbf{B}_I^{bT}(\mathbf{v}_e)\mathbf{M}(\mathbf{v}_e) \\
& + \mathbf{B}_I^{sT}(\mathbf{v}_e)\mathbf{Q}(\mathbf{v}_e)\, d\Omega - \int_{\Omega_e} \mathbf{N}_I^T \hat{\mathbf{t}}\, d\Omega \} .
\end{aligned} \tag{74}$$

The tangential stiffness matrix can be calculated from

$$\begin{aligned}
DG_e^h(\mathbf{v}_e, \delta\mathbf{v}_e)\Delta\mathbf{v}_e &= \sum_{I=1}^{nel}\sum_{K=1}^{nel} \delta\mathbf{v}_I^T [\int_{\Omega_e} \mathbf{B}_I^T(\mathbf{v}_e)\mathbf{D}\mathbf{B}_K(\mathbf{v}_e) d\Omega \\
&\qquad + \int_{\Omega_e} \mathbf{G}_{IK} d\Omega \;] \Delta\mathbf{v}_K \\
&= \delta\mathbf{v}_e^T [\mathbf{K}_{TeM} + \mathbf{K}_{Te\sigma}] \Delta\mathbf{v}_e = \delta\mathbf{v}_e^T \mathbf{K}_{Te} \Delta\mathbf{v}_e ,
\end{aligned} \tag{75}$$

with $\mathbf{B}_I = [\mathbf{B}_I^m,\ \mathbf{B}_I^b,\ \mathbf{B}_I^s]^T$.

The second term in eq.(75) – the geometrical matrix $\mathbf{K}_\sigma$ follows from the linearizations of the virtual strains. After multiplication with the work conjugate stress resultants, we obtain the terms for $\mathbf{G}_{IK}$ in $\mathbf{K}_\sigma$. The membrane part is given by

$$\delta\mathbf{v}_e^T \mathbf{K}_{\sigma(N)e} \Delta\mathbf{v}_e = \sum_{I=1}^{nel}\sum_{K=1}^{nel} [\delta\mathbf{u}_I, \delta\boldsymbol{\theta}_I]^T \int_{\Omega_e} \mathbf{G}_{IK}(m) d\Omega \begin{bmatrix} \Delta\mathbf{u}_K \\ \Delta\boldsymbol{\theta}_K \end{bmatrix} . \tag{76}$$

with

$$\mathbf{G}_{IK}(m) = \begin{bmatrix} \widehat{S}\,\mathbf{1}_{3x3} & \mathbf{o}_{3x3} \\ \mathbf{o}_{3x3} & \mathbf{o}_{3x3} \end{bmatrix} \tag{77}$$

and

$$\begin{aligned} \widehat{S} &= N^{\alpha\beta}\, N_{I,\alpha}\, N_{K,\beta} \\ &= N^{11}\, N_{I,1}\, N_{K,1} + N^{22}\, N_{I,2}\, N_{K,2} + N^{12}\,(\, N_{I,1}\, N_{K,2} + N_{I,2}\, N_{K,1}\,)\,. \end{aligned} \tag{78}$$

For the geometric stiffness matrix of the shear part we need the second variation of the shear strains. Based on the introduced shear strain field one obtains

$$\begin{bmatrix} \Delta\delta\tilde{\gamma}_{\xi 3} \\ \Delta\delta\tilde{\gamma}_{\eta 3} \end{bmatrix} = \frac{1}{2} \begin{bmatrix} (1-\eta)\Delta\delta\gamma_{\xi 3B} + (1+\eta)\Delta\delta\gamma_{\xi 3D} \\ (1-\xi)\Delta\delta\gamma_{\eta 3A} + (1+\xi)\Delta\delta\gamma_{\eta 3C} \end{bmatrix}, \tag{79}$$

with

$$\begin{aligned} \Delta\delta\gamma_{\eta 3A} &= \delta\bar{\mathbf{a}}_{\eta A} \cdot \Delta\mathbf{d}_A + \Delta\bar{\mathbf{a}}_{\eta A} \cdot \delta\mathbf{d}_A + \bar{\mathbf{a}}_{\eta A} \cdot \Delta\delta\mathbf{d}_A \\ \Delta\delta\gamma_{\xi 3B} &= \delta\bar{\mathbf{a}}_{\xi B} \cdot \Delta\mathbf{d}_B + \Delta\bar{\mathbf{a}}_{\xi B} \cdot \delta\mathbf{d}_B + \bar{\mathbf{a}}_{\xi B} \cdot \Delta\delta\mathbf{d}_B \\ \Delta\delta\gamma_{\eta 3C} &= \delta\bar{\mathbf{a}}_{\eta C} \cdot \Delta\mathbf{d}_C + \Delta\bar{\mathbf{a}}_{\eta C} \cdot \delta\mathbf{d}_C + \bar{\mathbf{a}}_{\eta C} \cdot \Delta\delta\mathbf{d}_C \\ \Delta\delta\gamma_{\xi 3D} &= \delta\bar{\mathbf{a}}_{\xi D} \cdot \Delta\mathbf{d}_D + \Delta\bar{\mathbf{a}}_{\xi D} \cdot \delta\mathbf{d}_D + \bar{\mathbf{a}}_{\xi D} \cdot \Delta\delta\mathbf{d}_D\,. \end{aligned} \tag{80}$$

After some algebra we end up with the shear part of the geometric stiffness matrix

$$\mathbf{G}_{IK}(s) = \begin{bmatrix} \mathbf{o}_{3x3} & \frac{1}{8}\mathbf{g}_{IK} \\ \frac{1}{8}\mathbf{g}_{KI}^{T} & \frac{1}{8}\tilde{\mathbf{g}}_{IK} \end{bmatrix} \tag{81}$$

with

$$\begin{aligned} \mathbf{g}_{11} &= -(1-\eta)Q^{\xi 3}\mathbf{W}_{3B} - (1-\xi)Q^{\eta 3}\mathbf{W}_{3A} \\ \mathbf{g}_{22} &= (1-\eta)Q^{\xi 3}\mathbf{W}_{3B} - (1+\xi)Q^{\eta 3}\mathbf{W}_{3C} \\ \mathbf{g}_{33} &= (1+\eta)Q^{\xi 3}\mathbf{W}_{3D} + (1+\xi)Q^{\eta 3}\mathbf{W}_{3C} \\ \mathbf{g}_{44} &= -(1+\eta)Q^{\xi 3}\mathbf{W}_{3D} + (1-\xi)Q^{\eta 3}\mathbf{W}_{3A} \\ \mathbf{g}_{12} &= -(1-\eta)Q^{\xi 3}\mathbf{W}_{3B} \\ \mathbf{g}_{13} &= \mathbf{o} \\ \mathbf{g}_{14} &= -(1-\xi)Q^{\eta 3}\mathbf{W}_{3A} \\ \mathbf{g}_{23} &= -(1+\xi)Q^{\eta 3}\mathbf{W}_{3C} \\ \mathbf{g}_{24} &= \mathbf{o} \\ \mathbf{g}_{34} &= (1+\eta)Q^{\xi 3}\mathbf{W}_{3D} \\ \mathbf{g}_{KI} &= -\mathbf{g}_{IK} \end{aligned} \tag{82}$$

and

$$\begin{aligned}
\tilde{\mathbf{g}}_{11} &= (1-\eta)Q^{\xi 3}\mathbf{A}_{\xi B} + (1-\xi)Q^{\eta 3}\mathbf{A}_{\eta A} \\
\tilde{\mathbf{g}}_{22} &= (1-\eta)Q^{\xi 3}\mathbf{A}_{\xi B} + (1+\xi)Q^{\eta 3}\mathbf{A}_{\eta C} \\
\tilde{\mathbf{g}}_{33} &= (1+\eta)Q^{\xi 3}\mathbf{A}_{\xi D} + (1+\xi)Q^{\eta 3}\mathbf{A}_{\eta C} \\
\tilde{\mathbf{g}}_{44} &= (1+\eta)Q^{\xi 3}\mathbf{A}_{\xi D} + (1-\xi)Q^{\eta 3}\mathbf{A}_{\eta A} \\
\tilde{\mathbf{g}}_{12} &= (1-\eta)Q^{\xi 3}\mathbf{A}_{\xi B} \\
\tilde{\mathbf{g}}_{13} &= \mathbf{o} \\
\tilde{\mathbf{g}}_{14} &= (1-\xi)Q^{\eta 3}\mathbf{A}_{\xi A} \\
\tilde{\mathbf{g}}_{23} &= (1+\xi)Q^{\eta 3}\mathbf{A}_{\xi C} \\
\tilde{\mathbf{g}}_{24} &= \mathbf{o} \\
\tilde{\mathbf{g}}_{34} &= (1+\eta)Q^{\xi 3}\mathbf{A}_{\xi D} \\
\tilde{\mathbf{g}}_{KI} &= \tilde{\mathbf{g}}_{IK}
\end{aligned} \tag{83}$$

where

$$\begin{aligned}
\mathbf{W}_{3M} &= \bar{\mathbf{t}}_{1M} \otimes \bar{\mathbf{t}}_{2M} - \bar{\mathbf{t}}_{2M} \otimes \bar{\mathbf{t}}_{1M} \\
\mathbf{A}_{\xi M} &= \tfrac{1}{2}(\mathbf{d}_M \otimes \bar{\mathbf{a}}_{\xi M} + \bar{\mathbf{a}}_{\xi M} \otimes \mathbf{d}_M) - (\bar{\mathbf{a}}_{\xi M} \cdot \mathbf{d}_M)\mathbf{1} \quad .
\end{aligned} \tag{84}$$

The bending part $\mathbf{G}_{IK}(b)$ is then defined by

$$\mathbf{G}_{IK}(b) = \begin{bmatrix} \mathfrak{O}_{3\times 3} & \mathbf{g}_{u\theta} \\ \mathbf{g}_{\theta u} & \mathbf{g}_{\theta\theta} \end{bmatrix} \tag{85}$$

with the submatrices

$$\begin{aligned}
\mathbf{g}_{u\theta} &= \tfrac{1}{2}M^{\alpha\beta}\,[\; N_{I,\alpha}\mathbf{W}_3 N_{K,\beta} + N_{I,\alpha}\mathbf{W}_\beta N_K \\
&\qquad + N_{I,\beta}\mathbf{W}_3 N_{K,\alpha} + N_{I,\beta}\mathbf{W}_\alpha N_K \;] \\
\mathbf{g}_{\theta u} &= \tfrac{1}{2}M^{\alpha\beta}\,[\; N_{I,\beta}\mathbf{W}_3^T N_{K,\alpha} + N_I\mathbf{W}_\beta^T N_{K,\alpha} \\
&\qquad + N_{I,\alpha}\mathbf{W}_3^T N_{K,\beta} + N_I\mathbf{W}_\alpha^T N_{K,\beta} \;] \\
\mathbf{g}_{\theta\theta} &= \tfrac{1}{2}M^{\alpha\beta}\,[\; N_{I,\beta}\mathbf{A}_\alpha N_K + N_I\mathbf{A}_\alpha N_{K,\beta} + N_I\mathbf{A}_{\alpha\beta}N_K \\
&\qquad + N_{I,\alpha}\mathbf{A}_\beta N_K + N_I\mathbf{A}_\beta N_{K,\alpha} + N_I\mathbf{A}_{\beta\alpha}N_K \;] .
\end{aligned} \tag{86}$$

The complete representation of the geometrical matrix is an essential condition for a quadratical convergence behaviour within the Newton iteration. The residual and the tangent stiffness matrix are integrated numerically using a 2×2 quadrature.

The shear strains are introduced with respect to $\xi_\alpha = \xi, \eta$. A transformation to Θ_β is shown in eq. (57) and bases on the introduction of the Jacobian $\mathbf{J}$, defined in eq. (55). It holds

$$\boldsymbol{\gamma} = \mathbf{J}^{-1}\tilde{\boldsymbol{\gamma}}, \qquad \begin{bmatrix} \gamma_{13} \\ \gamma_{23} \end{bmatrix} = \mathbf{J}^{-1}\begin{bmatrix} \gamma_{\xi 3} \\ \gamma_{\eta 3} \end{bmatrix} . \tag{87}$$

The internal virtual work, restricted to the shear terms is defined by

$$D\,\pi_s \cdot \delta\mathbf{v} = \int_\Omega \delta\boldsymbol{\gamma} \cdot \mathbf{Q}\, d\Omega = \int_\Omega \delta\boldsymbol{\gamma}^T \mathbf{D}^s \boldsymbol{\gamma}\, d\Omega \tag{88}$$

and with eq.(87) the shear part is transformed to

$$D\,\pi_s \cdot \delta\mathbf{v} = \int_\Omega \delta\tilde{\gamma}^T \mathbf{J}^{-T}\mathbf{D}^s\mathbf{J}^{-1}\tilde{\gamma}\,d\Omega = \int_\Omega \delta\tilde{\gamma}^T \tilde{\mathbf{D}}^s\tilde{\gamma}\,d\Omega = \int_\Omega \delta\tilde{\gamma}^T \tilde{\mathbf{Q}}\,d\Omega\,. \quad (89)$$

Thus the formulation of the shear term can be performed in the local ξ, η – coordinate systems with $\tilde{\mathbf{D}}^s = \mathbf{J}^{-T}\mathbf{D}^s\mathbf{J}^{-1}$.

The components of the axial vector $\boldsymbol{\theta}$ have been introduced in $(58)_2$ with respect to the Cartesian basis system $\mathbf{e}_i$. Thus up to now we have three global rotational parameters. Since there is no bending stiffness with respect to the shell normal in differentiable surfaces we eliminate the drilling degree of freedom. The virtual axial vector $\delta\boldsymbol{\theta}_I$ of node I can be decomposed as

$$\delta\boldsymbol{\theta}_I = \delta\theta_{Ij}\mathbf{e}_j = \delta\beta_{I\alpha}\bar{\mathbf{t}}_{I\alpha} \quad (90)$$

With (90) two local rotational parameters $\delta\beta_{I\alpha}$ are introduced. The drilling degree of freedom $\delta\beta_{I3}$ is assumed to be zero. Equation (90) can be written in matrix notation

$$\delta\boldsymbol{\theta}_I = \begin{bmatrix} \bar{\mathbf{t}}_{I1} & \bar{\mathbf{t}}_{I2} \end{bmatrix}_{(3x2)} \begin{bmatrix} \delta\beta_{I1} \\ \delta\beta_{I2} \end{bmatrix}_{(2x1)}$$

$$\delta\boldsymbol{\theta}_I = \mathbf{T}_I\delta\boldsymbol{\beta}_I \quad . \quad (91)$$

This transformation and the associated one for node K $\quad \Delta\boldsymbol{\theta}_K = \mathbf{T}_K\Delta\boldsymbol{\beta}_K$ are inserted into the linearized virtual work principle given in (74) and (75)

$$DG_e^h(\bar{\mathbf{v}}_e, \delta\mathbf{v}_e)\Delta\mathbf{v}_e + G_e^h(\mathbf{v}_e, \delta\mathbf{v}_e) =$$

$$\sum_{I=1}^{nel}\sum_{K=1}^{nel} [\delta\mathbf{u}_I, \delta\boldsymbol{\theta}_I]^T \left\{ \begin{bmatrix} \mathbf{K}_{uu} & \mathbf{K}_{u\theta} \\ \mathbf{K}_{u\theta} & \mathbf{K}_{\theta\theta} \end{bmatrix}_{(6x6)} \begin{bmatrix} \Delta\mathbf{u}_K \\ \Delta\boldsymbol{\theta}_K \end{bmatrix}_{(6x1)} + \begin{bmatrix} \mathbf{G}_{uI} \\ \mathbf{G}_{\theta I} \end{bmatrix} \right\} \quad (92)$$

which leads to

$$DG_e^h(\mathbf{v}_e, \delta\mathbf{v}_e)\Delta\mathbf{v}_e + G_e^h(\mathbf{v}_e, \delta\mathbf{v}_e) =$$

$$\sum_{I=1}^{nel}\sum_{K=1}^{nel} [\delta\mathbf{u}_I, \delta\boldsymbol{\beta}_I]^T \left\{ \begin{bmatrix} \mathbf{K}_{uu} & \mathbf{K}_{u\theta}\mathbf{T}_K \\ \mathbf{T}_I^T\mathbf{K}_{u\theta} & \mathbf{T}_I^T\mathbf{K}_{\theta\theta}\mathbf{T}_K \end{bmatrix}_{(5x5)} \begin{bmatrix} \Delta\mathbf{u}_K \\ \Delta\boldsymbol{\beta}_K \end{bmatrix}_{(5x1)} + \begin{bmatrix} \mathbf{G}_{uI} \\ \mathbf{T}_I^T\mathbf{G}_{\theta I} \end{bmatrix} \right\} . \quad (93)$$

The submatrices and vectors associated with the rotational degrees of freedom have to be transformed using $\mathbf{T}_I$ and $\mathbf{T}_K$. The elimination of the drilling degree of freedom is only performed at nodes in differentiable surfaces. Along intersections of shellparts we use the original three global parameters $\Delta\theta_{Ij}$. With this method we are able to compute folded plate structures (see also [SIM90], Part VII).

Remark 3:

1. The formulation of the Bathe/Dvorkin approach used in this element is similar to that described in [SIM90] and [IBR95]. Differences occur in all terms, describing the rotational behaviour due to the different approach of describing finite rotations. Furthermore this approach is described for the degenerated shell element of Ramm [RAM77],[RAM76] in [STM89].

2. The formulation of the Bathe/Dvorkin approach is given here with respect to the local ξ_α–system. Thus shear strains and shear forces have to be transformed to the global directions Θ_α using the transformation $\mathbf{Q} = \mathbf{J}^T \tilde{\mathbf{Q}}$ for an output of these values.

6 Examples

The developed element has been implemented in an extended version of the finite element program **FEAP**. A description of this program can be found in [ZIT89].

We show three types of examples. First of all we show the ability of our element to describe finite rotations in standard linear elastic test problems, then we give examples for composite shells with finite rotations and finally we discuss the application of the element to a dynamic problem.

Clamped spherical rubber shell

The nonlinear behaviour of a clamped spherical shell of rubber like material has been analyzed by Taber [TAB82] experimentally and analytically. This solution does not take into account shear deformations. The system and material data are

$$E = 4000\,\text{kPa} \quad \nu = 0.5 \quad R = 26.3\,\text{mm} \quad h = 4.4\,\text{mm}$$

and the finite element mesh is shown in Figure 4.

The shell is analyzed using one quadrant with a 16x16 finite element mesh. We increase the shear correction factor κ by a factor of 100 to suppress the shear deformations, see [SIM90]. A theoretical background for this technique is that the shear term in the tangent stiffness matrix can be used as a penalty term for a Kirchhoff–type theory, see e.g. [ZIT89].

Figure 5 shows different load–deflection curves for this problem. There is an excellent agreement between experimental and computed results. The results of the present formulation differ slightly from that published in [SIM90], which may depend on the different membrane interpolation. In addition the results of an axisymmetric shell element with finite rotations, see [WAG90], are depicted in the Figure.

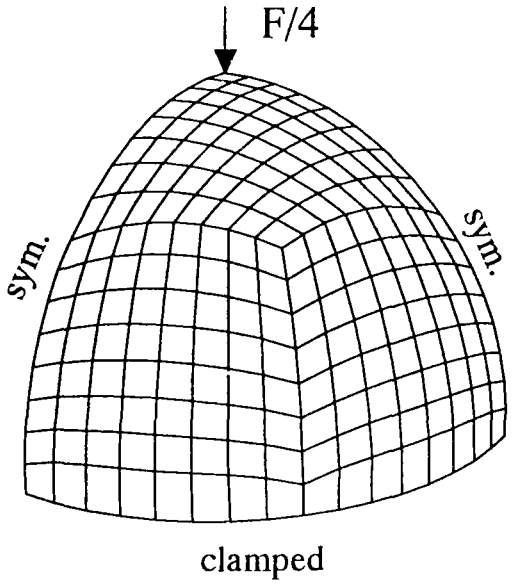

Figure 4: *Spherical rubber shell under point load*

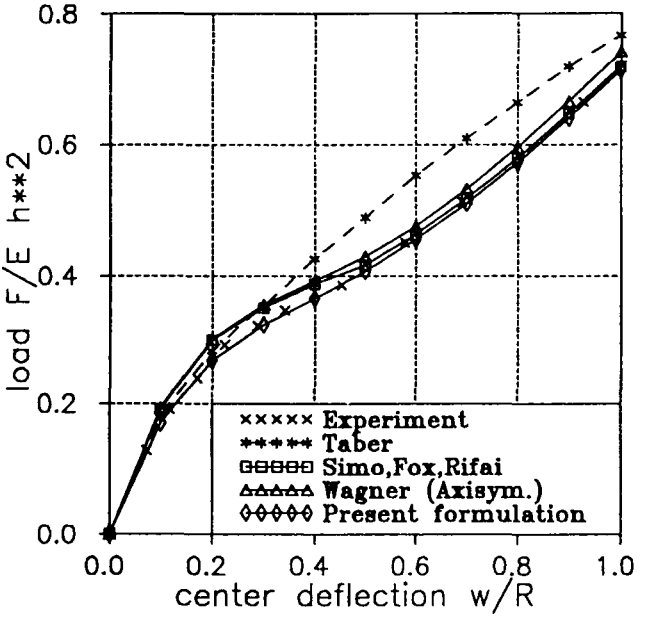

Figure 5: *Normalized load deflection curves for a rubber shell*

The calculations are performed in 10 displacement controled steps. Applying this solution strategy the calculation of the entire load-displacement curve can be done in an efficient way. The Newton-type convergence behaviour is shown in table 1 for the norm $||\mathbf{G}||_2$ of the residual for some displacement increments. The final deformed system at a deflection w=R is shown in Figure 6.

disp	w/R	0.1	0.4	0.7	1.0
norm	1	$1.18E+06$	$1.13E+06$	$1.08E+06$	$1.07E+06$
$\|\|\mathbf{G}\|\|_2$	2	$3.57E+04$	$4.71E+04$	$5.82E+04$	$7.81E+04$
in	3	$7.55E+02$	$1.44E+03$	$1.38E+03$	$1.94E+03$
iter-	4	$2.65E+02$	$6.11E+01$	$4.40E+01$	$1.63E+02$
ation	5	$3.74E-02$	$3.53E-02$	$3.53E-02$	$3.67E-02$
no.	6	$1.09E-07$	$8.97E-08$	$1.97E-08$	$1.21E-07$
load	F/Eh^2	0.170	0.364	0.511	0.713

Table 1 Convergence behaviour for spherical rubber shell

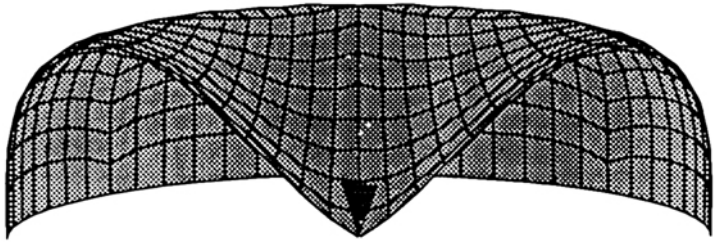

Figure 6: *Spherical rubber shell under point load, deformed mesh at w/R=1*

Clamped cylindrical Composite shell

The nonlinear behaviour of a clamped cylindrical shell panel of composite material subjected to a uniform load for a cross ply $[0°, 90°]$ has been analyzed in [RCH85] using a displacement finite element model based on the von Kármán equations. The material and geometrical data are

$$\begin{array}{llllll} E_1 = 25 \cdot 10^6 \text{ psi} & G_{12} = 0.5 \cdot 10^6 \text{ psi} & R = 2540 \text{ in} \\ E_2 = 1 \cdot 10^6 \text{ psi} & G_{13} = 0.5 \cdot 10^6 \text{ psi} & a = 254 \text{ in} \\ \nu = 0.25 & G_{23} = 0.2 \cdot 10^6 \text{ psi} & h = 2.54 \text{ in} . \end{array}$$

The system is depicted in Figure 7.

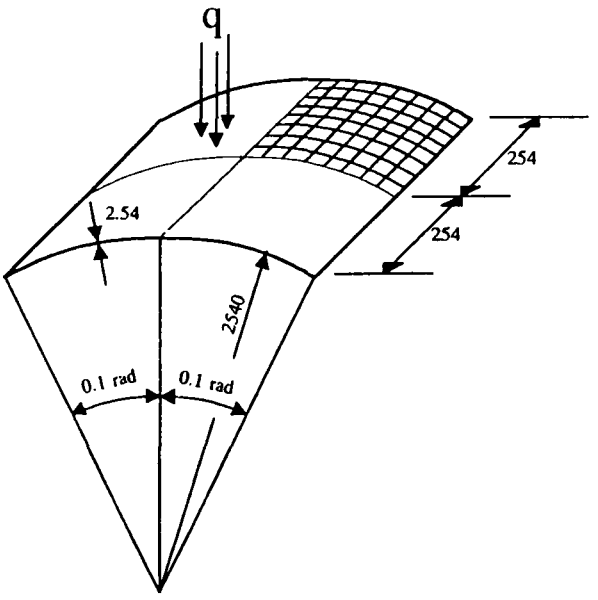

Figure 7: *Cylindrical composite shell panel*

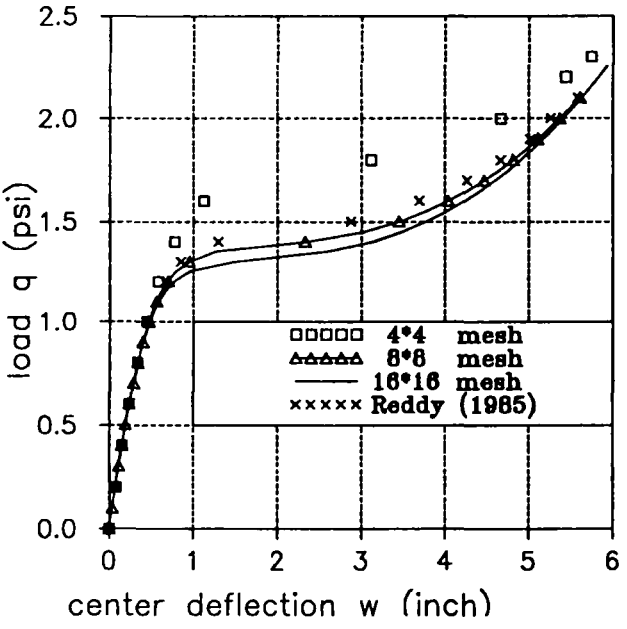

Figure 8: *Load deflection curves for a cylindrical shell segment under uniform load*

We run this example to test the composite formulation of our element. In this example finite rotations do not occur. The load deflection curves for the uniform load versus the center deflection are depicted in Figure 8 for 4*4, 8*8 and a 16*16 finite element mesh for one quarter of the shell.

Due to the boundary conditions a certain number of elements is necessary to produce accurate results, especially in the region where we have large changes in the center displacement at nearly constant external loads. The results differ slightly from that given in [RCH85]. A further discussion is not possible because in [RCH85] no information is given on the element formulation and the finite element meshes.

Hyperboloidal Shell under two pairs of opposite loads

There exist a number of benchmark problems for shell element formulations in the geometrical linear and nonlinear case. One example is a hemispherical shell under two opposite pairs of loads, see e.g. [MCH85]. Based on this example Başar et.al. [BDM92] define a similar problem for a hyperboloidal shell with and without composite material behaviour. Here we want to discuss the composite hyperboloidal shell. Due to the symmetry only one eighth of the shell has to be discretized. The shell has been analyzed for two sets of laminate schemes. Both are of cross ply type with $[0°, 90°, 0°]$ and $[90°, 0°, 90°]$. Here 90° means a fiber orientation into the circumferential direction.

The geometrical and material parameters chosen in [BDM92] are

$$\begin{array}{llllllll} E_1 = 40 \cdot 10^6 & G_{12} = 0.6 \cdot 10^6 & h = 0.12 & R_1 = 7.5 \\ E_2 = 1 \cdot 10^6 & G_{13} = 0.6 \cdot 10^6 & h_i = 0.04 & R_2 = 15.0 \\ \nu = 0.25 & G_{23} = 0.6 \cdot 10^6 & P = 5 & H = 20.0 \end{array}$$

The radius of the hyperboloidal shell is described by $R(x_3) = \frac{R_1}{c}\sqrt{c^2 + (x_3)^2}$ with $c = \frac{20}{\sqrt{3}}$. One eighth of the shell is depicted in Figure 9.

Results are shown for points A,B,C and D of the shell, see Figure 9 for both types of layer sequences. Large displacements and finite rotations occur within the nonlinear load deflection regime. A path following scheme, see e.g. [WAW88] may be used but is not necessary. Especially for the second layer sequence the path following method is advantageous due to the extremely weak behaviour of the shell for low values of the external loads. In the Figures 10 and 11 we show the load deflection curves for the sequence $[0°, 90°, 0°]$ and a finite element mesh with 16*16 elements. The results are in good agreement with those calculated in [BDM92] based on a 28 * 28 finite element mesh.

In the Figures 12 and 13 the load deflection curves for the layer sequence $[90°, 0°, 90°]$ based on a 16*16 element mesh are depicted. Slightly differences occur in the presence of large displacements for the curves $\lambda - u_A$, $\lambda - u_C$. If we use a 28*28 mesh too the results nearly coincide with those in [BDM92].

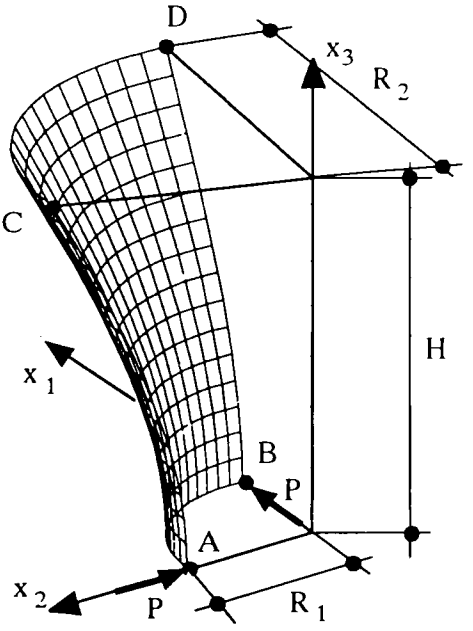

Figure 9: *Hyperboloidal composite shell*

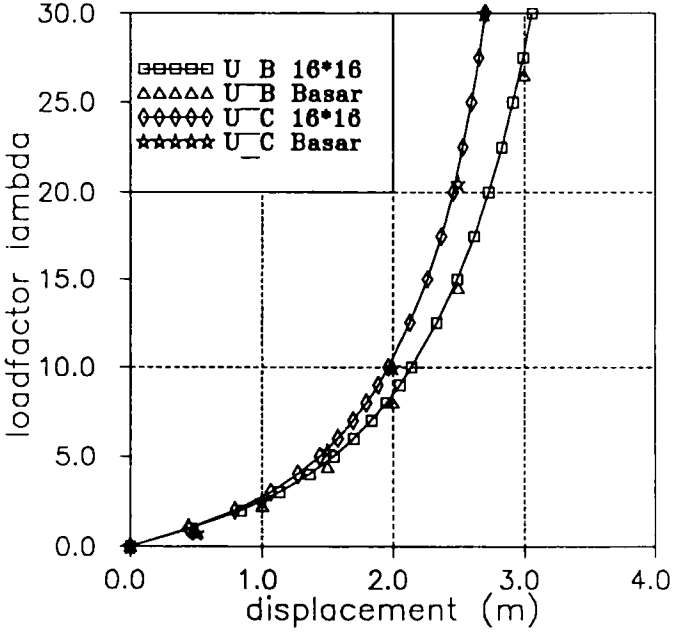

Figure 10: *Hyperboloidal composite shell* $[0°, 90°, 0°]$, $\lambda - u_B$, $\lambda - u_C$

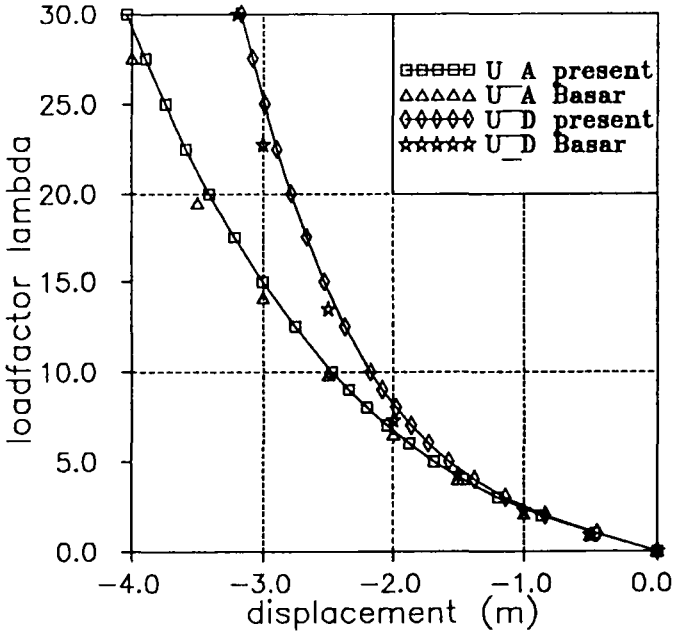

Figure 11: *Hyperboloidal composite shell* $[0°, 90°, 0°]$, $\lambda - u_A$, $\lambda - u_D$

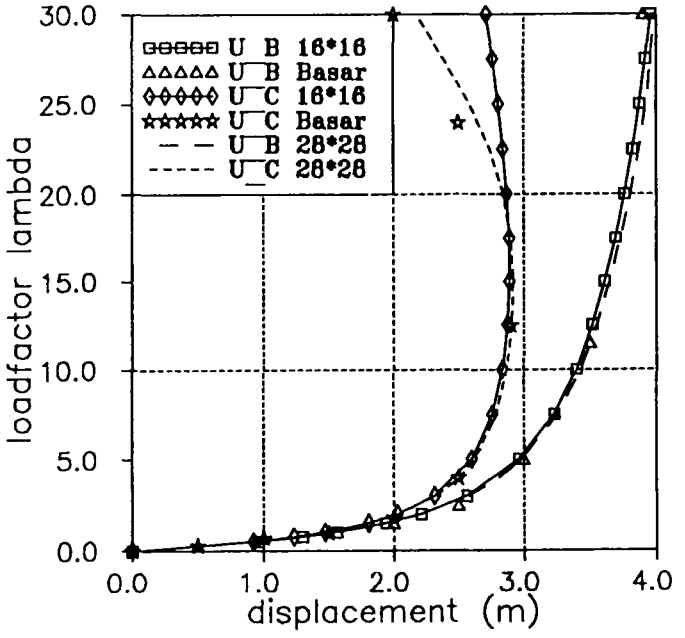

Figure 12: *Hyperboloidal composite shell* $[90°, 0°, 90°]$, $\lambda - u_B$, $\lambda - u_C$

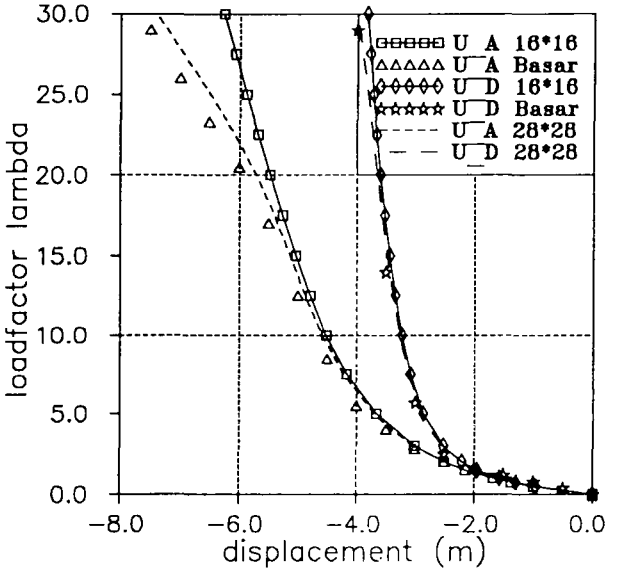

Figure 13: *Hyperboloidal composite shell* $[90°, 0°, 90°]$, $\lambda - u_A$, $\lambda - u_D$

In the following Figures we show the deformed meshes at a load level of $\lambda = 30$. Based on the undeformed system in Figure 9 the deformed meshes are shown in the $x_1 - x_3$ plane and in $x_2 - x_3$ plane in the Figures 14 and 15. Furthermore the Figures 16 and 17 show perspective views of the deformed hyperboloidal shells.

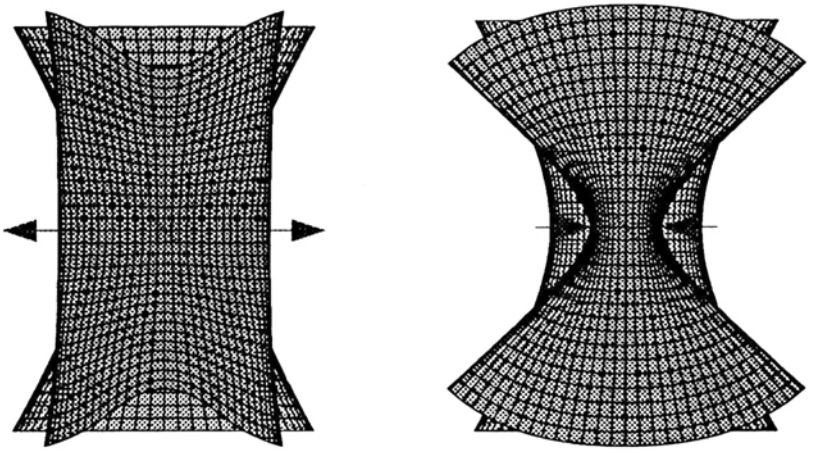

Figure 14: *Hyperboloidal composite shell* $[0°, 90°, 0°]$ - *deformed mesh in the* $x_1 - x_3$ *plane and* $x_2 - x_3$ *plane*

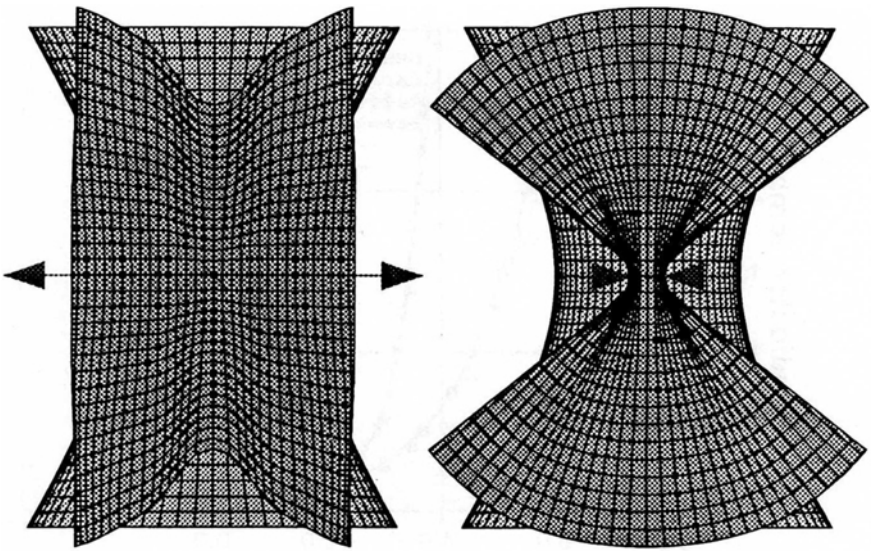

Figure 15: *Hyperboloidal composite shell* $[90°, 0°, 90°]$ - *deformed mesh in the* $x_1 - x_3$ *plane and* $x_2 - x_3$ *plane*

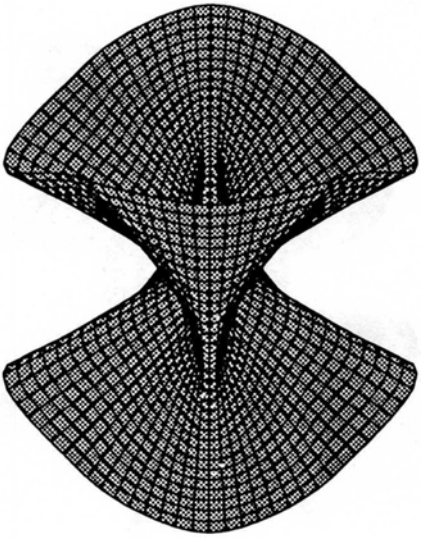

Figure 16: *Hyperboloidal composite shell* $[0°, 90°, 0°]$ - *deformed mesh, perspective view*

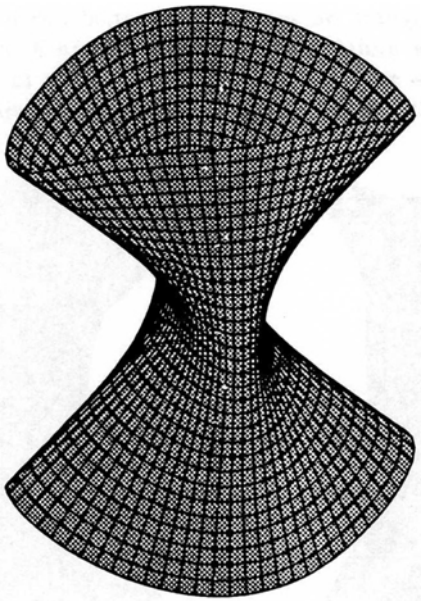

Figure 17: *Hyperboloidal composite shell* $[90°, 0°, 90°]$ - *deformed mesh, perspective view*

Rotation of a propfan–blade

This example has been chosen to demonstrate the ability of our element to describe finite rotations without difficulties. We discuss the rotation of a propfan blade under a time dependent axial moment.

It is characterized by the large number (8–10) of low–aspect–ratio highly swept blades which are twisted along the span and curved back about the axis of rotation. A typical example is the Hamilton–Standard SR3–propfan with a diameter of 2.70 m, shown in Figure 18.

Lammering [LAM90] has analyzed the Hamilton–Standard SR3–propfan. He discussed the behaviour of blades for different materials under centrifugal forces and a constant rotational speed. Furthermore he investigated the influence of the fiber orientation on the tip displacement of the blade and on the twisting at a certain point via optimization procedures.

Due to the symmetry of the system it is sufficient to analyze only one blade. Figure 19 shows two views of the blade. The rotation of the blade occurs around the 3–axis. For this purpose the blade is connected to the axis via rigid elements. The finite element discretization is defined by 798 nodes, 740 shell elements and 3990 degrees of freedom.

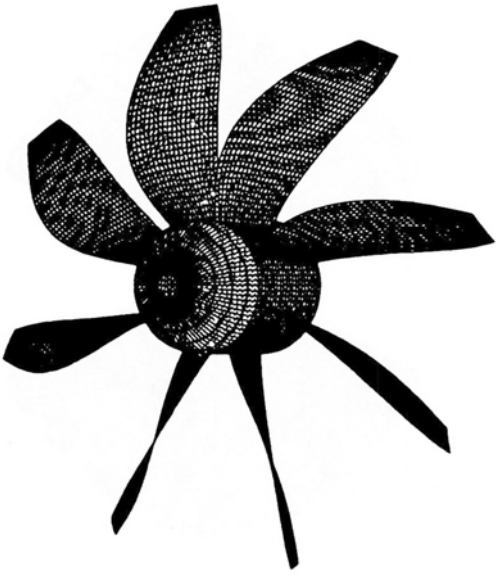

Figure 18: *Hamilton-Standard SR3-propfan*

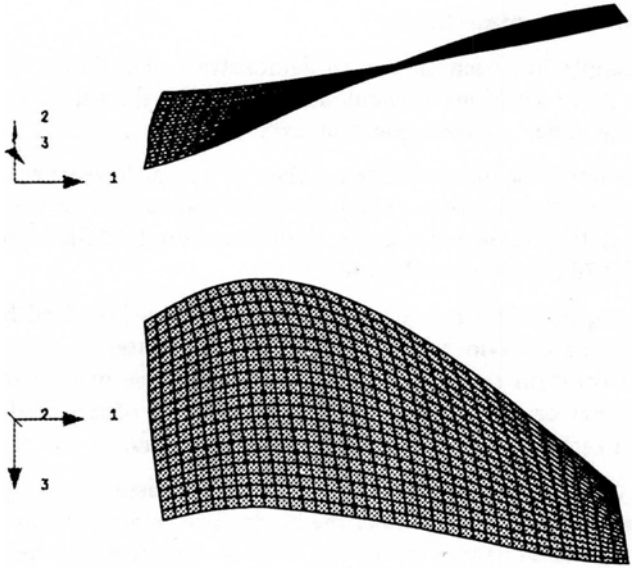

Figure 19: *Two views of the FE-mesh of the SR3-propfan*

The blade has a variable thickness. Within the finite element discretization the thickness h can be computed using $h^h = \sum_{I=1}^{nel} N_I h_I$ with the shape functions N_I and the nodal values of the thickness h_I. The thickness distribution is shown in Figure 20.

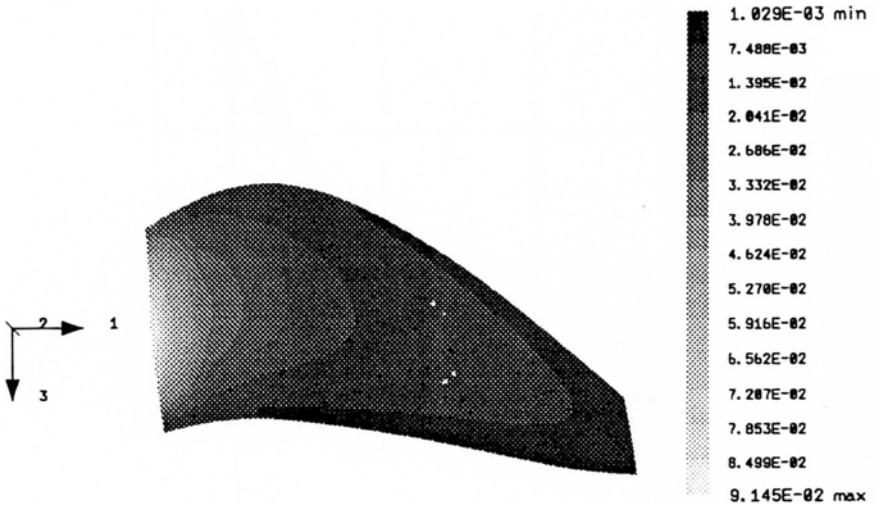

Figure 20: *SR3-propfan: distribution of thickness in m*

We choose 6 composite layers of constant thickness (0.8 mm), three at the top and three at the bottom of the blade. Thus the distance ζ_s^k between the midpoint of the considered layer and the reference surface has to be modified, see eq. (34). The fiber angle sequence $[90°, 45°, 0°, 0°, 45°, 90°]$ is symmetric. The angles are defined with respect to axis 3, see Figure 19.

The material data are chosen as follows

$$E_1 = 13500\,kN/cm^2 \quad G_{12} = 540kN/cm^2 \qquad \nu = 0.3$$
$$E_2 = 1000\,kN/cm^2 \qquad\qquad\qquad \rho = 1600kg/m^3\ .$$

In this example we discuss the motion of one rotor blade with initial conditions $\dot{\mathbf{x}} = \ddot{\mathbf{x}} = \mathbf{0}$. The motion is initialized through an axial moment $M_{33} = M_0\,t$, with $M_0 = 1kN\,cm/sec$ and the process time t in *seconds*.

A standard Newmark algorithm without damping is used. Within the nonlinear shell element a simple row sum technique leads to a lumped mass matrix, see e.g. [HUG87].

The results for the axis angle (angle around axis 3) versus time are depicted in Figure 21 for different time steps. Within this time the blade rotates three times.

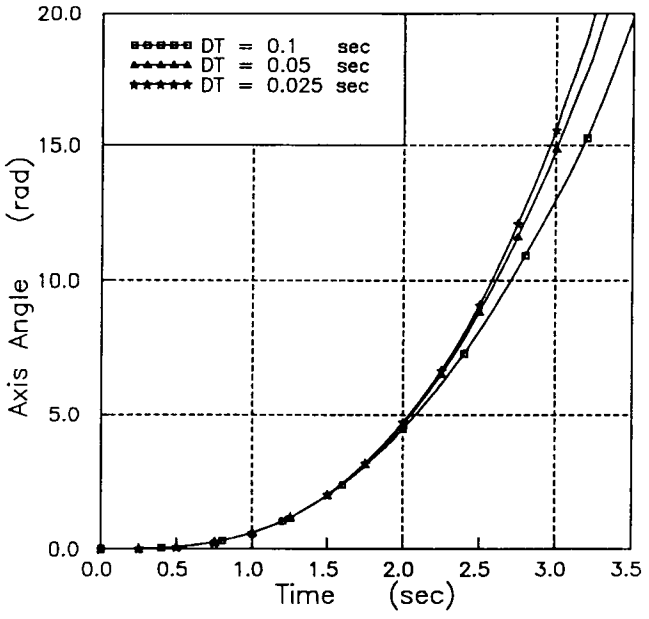

Figure 21: *Motion of the SR3-propfan, axis angle versus time*

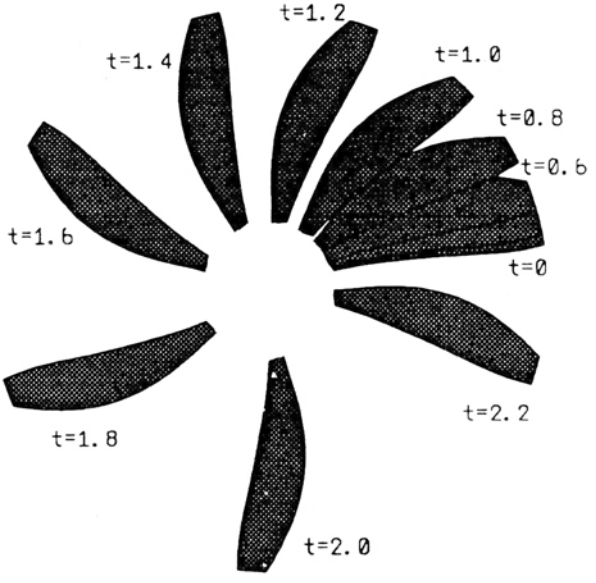

Figure 22: *Motion of the SR3-propfan, t = 0 - 2.2 sec, Δ t = 0.2 sec.*

Furthermore the deformed meshes are shown for t = 0–2.2 seconds in steps of 0.2 secs in Figure 22 (0.2,0.4,....2.2) and for t = 2.2-2.9 seconds in steps of 0.2 secs in Figure 23 (2.3,2.5,2.7,2.9).

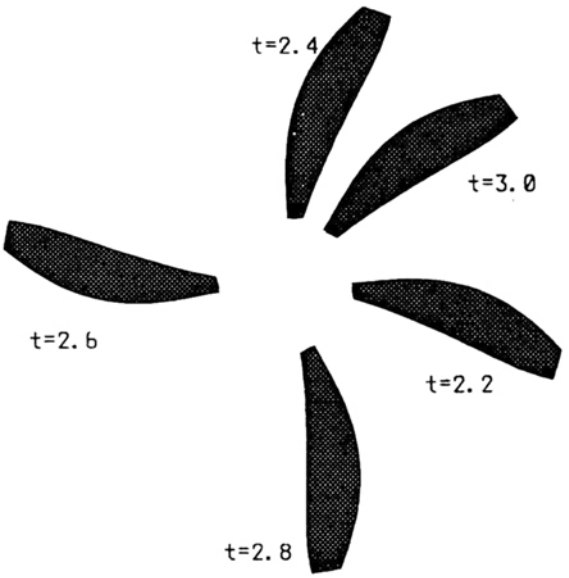

Figure 23: *Motion of the SR3-propfan, t = 2.3 - 2.9 sec,Δ t = 0.2 sec.*

It can be seen that the motion is nearly a rigid body motion. The example demonstrates the ability of the element to describe finite rotations. Here we have more than 3 rotations. Thus the rotation angles are up to 1150 degrees.

7 Conclusions

In this paper we have derived a finite element formulation for geometrical nonlinear shell structures. The formulation bases on a direct introduction of the isoparametric finite element formulation into the shell equations. The element allowes the occurence of finite rotations which are described by a rotation tensor. A layerwise linear elastic material model for composites has been chosen. The consistent linearization of all equations leads to quadratic convergence behaviour within the nonlinear solution procedure. Examples show the applicability and effectivity of the developed element.

References

[SIM90] Simo, J. C., Fox, D.D., Rifai, M. S., On a Stress Resultant Geometrically Exact Shell Model, *Comp. Meth. Appl. Mech. Engng.* (Part I: **72** 267–304 (1989), Part II: **73** 53–92 (1989), Part III: **79** 21–70 (1990), Part VII:**108** 319–339 (1993))

[WAS93] Wagner W., Stein E., A New Finite Element Formulation for Cylindrical Shells of Composite Material, *Composites Engineering*, **3**, 899–910 (1993)

[RAM77] Ramm, E., A Plate/Shell Element for Large Deflections and Rotations, *US–Germany Symp. on 'Formulations and Computational Algorithms in Finite Element Analysis'*, M.I.T.–Press, Boston, 264–293 (1977)

[RAM76] Ramm, E., *Geometrisch nichtlineare Elastostatik und Finite Elemente*, Report No. 76-2, Inst. f. Baustatik Universität Stuttgart 1976

[TSA88] Tsai, W. S., *Composites Design*, Think Composites, Dayton (1988)

[BUR92] Büchter N., Ramm E., Shell theory versus degeneration - A comparison in large rotation finite element analysis , *Int. J. Num. Meth. Engng.* **34** 39–59 (1992)

[PIE77] Pietraszkiewicz, W., Introduction to the Non-linear Theory of Shells, Techn. Rep. Inst. f. Mechanik, Nr. 10, Ruhr-Universität Bochum (1977)

[BAD85] Bathe, K.J., Dvorkin, E.N., A 4–Node Plate Bending Element based on Mindlin/Reissner Theory and a Mixed Interpolation, *Int. J. Num. Meth. Engng.* **21** 367–383 (1985)

[DVB84] Dvorkin, E.N. , Bathe,K.J., A Continuum Mechanics based Four–Node Shell Element for General Nonlinear Analsysis, *Engng. Comp.* 1 77–88 (1984)

[ZIT89] Zienkiewicz, O. C. and Taylor R. L., *The Finite Element Method*, Vol.1-2, 4. Edn. Mc Graw–Hill, London (1989/1991)

[RAM86] Ramm, E., Matzenmiller, A., Large deformation shell analysis based on the degeneration concept, *Finite Element methods for Plate and Shell Structures* (Eds. Hughes,T.J.R., Hinton, E.) Pineridge Press, Swansea 365–393 (1986)

[STM89] Stander,N., Matzenmiller, A., Ramm, E., An assessment of Assumed Strain Methods in Finite Rotation Shell Analysis, *Engng. Comp.* **6** 57–66 (1989)

[IBR95] Ibrahimbegović A., On Assumed Shear Strain in Finite Rotation Shell Analysis, *Engng. Comp.* **11** in press (1995)

[TAB82] Taber, L.A., Large Deflection of a Fluid–Filled Spherical Shell under a Point Load, *J. Appl. Mech., Trans. ASME Ser. E*, **39**, 121–128 (1982)

[WAG90] Wagner, W., A Finite Element Model for Nonlinear Shells of Revolution with Finite Rotations, *Int. J. Num. Meth. Engng.* **29** 1455–1471 (1990)

[MCH85] McNeal, R. H., Harder, R. L., A proposed standard set of problems to test finite element accuracy. *J. of Finite Elements in Analysis & Design* **1** 3–20 (1985)

[HUL81] Hughes, T.J.R., Liu, W.K., Nonlinear Finite Element Analysis of Shells. *Comp. Meth. Appl. Mech. Engng.* Part I: Three–dimensional shells, **26** 331–362 (1981) Part II: Two–dimensional shells, **27** 167–181 (1981)

[SPH86] Stanley, G. M., Park, K.C., Hughes, T.J.R., Continuum–based resultant shell elements, *Finite Element methods for Plate and Shell Structures* (Eds. Hughes, T.J.R., Hinton, E.) Pineridge Press, Swansea, 1–45 (1986)

[GSW89] Gruttmann, F., Stein, E., Wriggers, P., Theory and Numerics of Thin Elastic Shells with Finite Rotations, *Ing. Archiv* **59** 54–67 (1989)

[IBR94] Ibrahimbegović A., Frey F., Stress Resultant Geometrically Nonlinear Shell Theory With Drilling Rotations, *Comp. Meth. Appl. Mech. Engng.* (Part I: **118** 265–284 (1994), Part II: **118** 285–308 (1995))

[PAR91] Parisch, H., An Investigation of a Finite Rotation Four Node Shell Element, *Int. Num. Meth. Engng.* **31** 127–150 (1991)

[GEB90] Gebhardt H., *Finite Element Konzepte für schubelastische Schalen mit endlichen Drehungen*, Report No. 10, Inst. f. Baustatik, Universität Karlsruhe, 1990

[SCH86] Schoop, H., Oberflächenorientierte Schalentheorien endlicher Verschiebungen, *Ing.Archiv* **56** 427–437 (1986)

[BAD90] Başar, Y., Ding, Y., Theory and Finite-Element Formulation for Shell Structures undergoing Finite Rotations, *Advances in the Theory of Plates and Shells* (Eds. Voyiadjis, G.Z., Karamanlidis, D.) Elsevier Science Publishers, Amsterdam, 3–26 (1990)

[BDM92] Başar, Y., Ding, Y., Menzel, W., Montag, U., Finite Rotation Shell Elements via Finite–Rotation Shell Theories, Statik und Dynamik im konstruktiven Ingenieurbau, Festschrift Wilfried B. Krätzig, 1992

[DOR90] Dorninger, K., Rammerstorfer, F.G., A Layered Composite Shell Element for Elastic and Thermoelastic Stress and Stability Analysis at Large Deformations, *Int. Num. Meth. Engng.* **30** 833–858 (1990)

[RCH85] Reddy, J.N., Chandrashekhara, K., Nonlinear Analysis of Laminated Shells including Transverse Shear Strains, *AIAA Journal* **23** 440–441 (1985)

[WAW88] Wagner, W., Wriggers, P., A Simple Method for the Calculation of Postcritical Branches, *Engineering Computations*, **5** 103–109 (1988)

[WRG93] Wriggers, P., Gruttmann, F., Thin Shells with Finite Rotations formulated in Biot–Stresses: Theory and Finite Element Formulation *Int. Num. Meth. Engng.*, **36**, 2049–2071, 1993

[WRG90] Wriggers P., Gruttmann F., Large Deformations of Thin Shells: Theory and Finite-Element-Discretization, *Analytical and Computational Models of Shells* (Eds. Noor, A., Belytschko T., Simo, J. C.) ASME CED-Vol. 3, 135-159 (1990)

[PIJ87] Pinsky, P. M., Jang, J., A C^0–elastoplastic shell element based on assumed covariant strain interpolations, *NUMETA 1987, Numerical Methods in Engineering: Theory and Applications* (Eds. Pande, G.N., Middleton, J.) Pineridge Press, Swansea (1987)

[LAM90] Lammering, R., Structural Analysis and Optimization of a Propfan–Blade by use of the Finite Element Method, *Engineering Computations* **7** 327–337 (1990)

[HUG87] Hughes, T. J. R., *The Finite Element Method*, Prentice–Hall Inc., Englewood Cliffs, New Jersey (1987)